UNIVERSITAT POLITÈCNICA DE VALÈNCIA

School of Industrial Engineering

Characterisation of Base oils for E-fluid Applications Under Thermal and Electrical Degradation

Master's Thesis

Master's Degree in Chemical Engineering

AUTHOR: Telfer , Ben

Tutor: Tormos Martínez, Bernardo Vicente

ACADEMIC YEAR: 2022/2023

DEPARTMENT OF CHEMICAL & PROCESS ENGINEERING

University of Strathclyde Engineering

Department of Chemical & Process Engineering

MEng in Chemical & Process Engineering

18530

Characterisation of Base Oils for EV-fluid Applications Under Thermal and Electrical Degradation

Word Count: 12,624

This project is submitted in partial fulfilment of the regulations governing the award of Degree of MEng in Chemical Engineering at the University of Strathclyde

Name: **Ben Telfer** Date: **13/04/2023**

Organisation: **Universitat Politècnica de València (UPV)**

In-house Supervisor: **Prof. Bernardo V. Tormos Martinez**

Academic Supervisor: **Dr. Demosthenes Kivotides**

Executive Summary

The adoption of electric vehicles (EVs) is growing rapidly, and with the pressure of legislative emissions reduction targets the rate of growth is likely to increase significantly within the next decade. Therefore, it is imperative that the technological advancement of EVs keeps pace with demand to provide efficiency and practicality for consumers. One such technological aspect is the system for cooling EV batteries, which is especially important with the development of rapid charging, increasing battery capacities and high-performing vehicles. E-thermal fluids are coolants designed to come into direct contact with the battery cells and electronic components, establishing a more efficient and compact cooling system than indirect cooling alternatives.

This investigation aims to determine the suitability of selected base oils for e-thermal fluid applications by characterising their physical, thermal and electrical properties. API Group III mineral base oil (GIII), API Group IV polyalphaolefin (PAO), diester and polyolester are selected for testing. Fresh, thermally degraded and electrically degraded oil samples are tested to investigate the potential impacts of degradation that could occur during practical 'fill for life' applications in EVs. Accelerated synthetic degradation is achieved thermally by exposure to 150°C temperature for 120 hours and electrically by exposure to 1000 electrical breakdown discharges. Furthermore, infrared spectroscopy is performed to analyse the chemical compositions of the base oils and infer changes in molecular structure due to degradation that impact the measured properties.

The thermal and physical properties of viscosity, density, thermal conductivity and specific heat capacity were measured. Generally, degradation resulted in less than 2.5% change in these properties, except for thermal degradation of the PAO where 10.7% increase in viscosity and 3% decrease in specific heat capacity were observed. The Mouromtseff number was calculated as a figure of merit for heat transfer capability. The diester was found to have marginally better heat transfer properties than the other base oils, but each base oil showed suitable properties.

The electrical properties of dissipation factor, resistivity and breakdown voltage were measured. The PAO shows the lowest dissipation factor and highest resistivity, both of which are minimally impacted by degradation. While the ester oils are found to possess higher breakdown voltage than the PAO, their electrical properties are found to be negatively impacted by increased water content following electrical degradation. Furthermore, the ester oils have significantly lower resistivity and higher dissipation factor than both the PAO and GIII. Overall, it is concluded that the PAO has the most suitable properties for e-thermal fluid applications based purely on the properties characterised in this work. Further analysis is recommended to assess broader factors.

Table of Contents

Nomenclature List

Abbreviation	Definition
API	American Petroleum Institute
ASTM	American Society for Testing and Materials
BDV	Breakdown voltage
E-fluids	Electric vehicle fluids
EV	Electric vehicle
FTIR	Fourier-transform infrared
GIII	Mineral oil categorised as Group III according to API standards.
ICE	Internal combustion engine
IEC	International Electrotechnical Commission
KFC	Karl Fischer coulometric
LIB	Lithium-ion battery
Mo	Mouromtseff number
PAO	Polyalphaolefin
PCM	Phase change material
ppm	Parts per million
SE	Standard error
THW	Transient hot wire

List of Tables

List of Figures

Acknowledgements

I am grateful for the opportunity to carry out my master's thesis project at UPV, and I owe particular gratitude to the School of Industrial Engineering's international office for facilitating my registration and arrival at the university. I am greatly thankful to my project supervisor, Professor Tormos, for giving me the opportunity to carry out my project under his research group. His guidance, advice and feedback throughout the project have been greatly appreciated.

I would also like to thank my PhD mentor, Jorge Alvis, who took time out of his own research to provide me with guidance and support throughout the project. Jorge helped me to establish a clear scope for the work, provided training in the lab and was always available to give advice or answer questions. Furthermore, I must give thanks to Adbeel Balaguer Reyes, my other PhD mentor, who showed great patience in demonstrating how to use particular pieces of equipment and she was welcoming and supportive in the lab.

Further thanks must be given to my academic supervisor from Strathclyde, Dr Kivotides, who's comments and feedback were always constructive and valuable. I would also like to give thanks to all of the staff within the Chemical Engineering Department at Strathclyde, as it is with their tuition and guidance that I am able to write this thesis. I am especially grateful to the department for providing the opportunity to go on Erasmus exchange in my final semester, as the experience of living and studying in Valencia is one I will never forget. Again thanks are owed to Dr Kivotides as Erasmus Coordinator, for arranging the host university selection process, and I must also give final thanks to Kate Kenyon for dealing with the administration and paperwork that made the Erasmus exchange possible.

1 Introduction

1.1 Description of Institution

The work was carried out within the Universitat Politècnica de València (UPV), under their School of Industrial Engineering (ETSII). The UPV has established an excellent reputation as an institution for technical education over the past 50 years and, in 2022, was ranked as the top technological university in Spain [1]. The institution consists of 13 schools covering engineering, technology, art and science, and a student community of over 28,000.

The research was carried out in the Department of Thermal Engines and Machines (CMT), under the supervision of Prof. Bernardo Tormos. The CMT group has over 40 years of experience in research and postgraduate education, with over 100 members. With conventional research lines investigating the performance and efficiency of internal combustion engines, this work is developed under a series of new research lines investigating electric mobility – specifically battery thermal management and cooling system design.

1.2 Project Overview

In the past decade there has been a clear and focussed drive towards increasing the production and adoption of electric vehicles (EVs). In 2012, only 120,000 EVs were sold globally but by 2021 this quantity was surpassed in weekly EV sales – reaching a total of 16.5 million EVs on the roads [2]. The rapid growth in the EV market in recent years is largely due to the increase in public spending and development of policies that have incentivised and promoted the sale of EVs to reduce emissions from road transport [2,3]. Global road transport emissions were 5.86 Gt-CO_2 in 2021, contributing over 16% of all energy-related emissions [2]. Therefore, the transition from internal combustion engine (ICE) to battery powered vehicles is a clear and definable target for policy-makers to substantially cut emissions [4,5]. In June 2022, the European Parliament voted to amend EU regulation to ensure that all newly produced cars and vans produce zero emissions by 2035, and policies are being made globally to gradually restrict emissions from road vehicles [6]. With such policies, and the continued growth momentum of the EV market, the challenge remains for EV technology to keep pace with demand.

Effective lubrication and thermal management are crucial for both internal combustion engines and battery powered electric motors, with significant importance for reducing system degradation and improving power efficiency. Similar to conventional ICE vehicles, EVs require transmission oil and grease for lubrication of moving mechanical parts, however, EVs additionally require a thermal fluid to manage the temperature of the battery system [7]. For EVs, these fluids have specific requirements for their thermal and electrical properties and are collectively known as 'e-fluids'. This report will focus on e-thermal fluids which are essential for maintaining optimal battery temperature, providing homogeneous temperature of battery cells and coping with the thermal stress of rapid charging cycles [8]. Their capability to withstand the thermal and electrical stresses applied throughout the operating lifespan of the vehicle is imperative to the effective safety and performance of battery powered motors in EVs.

This investigation will compare the characteristics of four base-oils for application in e-thermal fluids: API Group III mineral oil (GIII), API Group IV polyalphaolefin (PAO), diester and polyolester. Conventional engine oil (5W30) will also be tested as a benchmark for the comparison. The aim is to investigate the effect of electrical and thermal degradation on the electrical, thermal and physical properties of the base oils to determine which would be most suitable for e-thermal fluid applications. The methods for electrical and thermal degradation aim to achieve accelerating aging of the fluids that emulate the degradation that may occur during the 10-20 year operating life of the fluid. The fluids will be characterised before and after degradation using a series of tests to measure their properties and spectroscopy will be used as an analysis tool to investigate the changes to the fluids' chemical structure. It should be noted that the term 'degradation' is used throughout this work to signify a process that can cause changes to the molecular structure of the oils and ultimately reduce the quality of their measured properties.

The following sections describe in more detail the context of the research and the experimental methods implemented before presentation of the results and discussion. Firstly, background information relevant to the research will be summarised to effectively contextualise the work. Similar studies will be briefly reviewed, and relevant technical theory will be explained. The methodology for base oil characterisation and degradation will then be described, including details of the laboratory equipment and relevant industry standards adopted. Results of the experimental analyses will then be presented and discussed in detail, before drawing relevant conclusions and proposing recommendations for future work.

1.3 Project Objectives

While the overarching aim of the project is to investigate the suitability of the properties of the selected base oils for e-thermal fluid applications, the work can be divided into the following specific objectives:

- To measure the Fourier-Transform Infrared (FTIR) absorbance spectrums of the fresh and degraded base oil samples, and from the results infer changes to the chemical structure of the oils that have occurred due to degradation such as oxidation. Together with measurement of the oil's water content, the FTIR results will be used to explain changes in the properties of the base oils after degradation.

- To measure and compare the thermal and physical properties of the fresh and degraded base oil samples, including density, viscosity, thermal conductivity and specific heat capacity. The Mouromtseff number will be calculated as a figure of merit for the heat transfer capability of the fluids.
- To measure and compare the electrical properties of the fresh and degraded oil samples, including dissipation factor, resistivity and breakdown voltage.
- To assess which base oils are most suitable for e-thermal fluid applications by constructing a qualitative decision matrix that ranks the oils based on various factors considering their properties and performance under degradation.

1.4 Learning Objectives

Beyond the project objectives outlined above, the following learning objectives set targets for the development of personal and technical skills:

- To experience living and studying in a foreign country, with the various challenges and rewards that come with meeting new people, learning a new language and adapting to a new culture.
- To continually improve my 'soft' skills by effectively communicating with my supervisors and research fellows, conveying complex and technical ideas clearly and concisely. Furthermore, the work will require effective time management, scheduling and organisation.
- To enhance my competence in practical laboratory work through training and hands-on experience with various pieces of technical equipment.
- To develop my knowledge and understanding in the growing sector of EV-fluids, and to effectively apply this knowledge to give my work context and meaning.
- To further develop my skills in data handling, analysis and presentation.

1.5 UN Sustainable Development Goals

It is important to emphasise this work's relation to the UN Sustainable Development Goals, as these goals provide a globally recognised framework for social, economic and environmental development. This work has particular relevance to the goals associated with climate action and reduction of harmful exhaust emissions. This work investigates EV-fluids in an attempt to promote the advancement of EV technology for better efficiency, drive range and practicality. In turn, this work contributes towards the wider-scale adoption of EVs which relates to 'Goal 11: Sustainable Cities and Communities' through the reduction of harmful emissions from internal combustion engine vehicles such as CO_2, NO_x and SO_2. Furthermore, with the intention for EV-fluids to be 'fill-for-life' this work promotes 'Goal 12: Responsible Consumption and Production' by reducing the current reliance on conventional engine oil that must be replaced frequently. Finally, the aforementioned factors are associated with 'Goal 13: Climate Action', with an increased proportion of EVs on the roads resulting in decreasing road transport exhaust emissions. EV-fluid technology must be advanced to allow for the gradual phasing-out of conventional internal combustion engine vehicles in the coming decades, cutting the associated CO_2 emissions and contributing to action against climate change.

2 Background

EVs require fluids for lubrication and thermal management, known collectively as e-fluids, and these must be developed to cater for a wide variety of EV designs and drivetrain configurations. When compared with the lubricating fluids for conventional ICE vehicles, e-fluids generally have a more complex set of conditions that their characteristics should adhere to, and this presents a challenge for their development.

2.1 EV Fluids for Lubrication & Thermal Management

Conventional ICE vehicles require three types of lubricants: engine oil, transmission fluid and grease. Engine oil plays various roles in the lubrication, cooling and cleaning of mechanical engine parts, and is typically replaced twice a year [9,10]. Transmission fluid is required for lubrication and hydraulic functions within the drivetrain (including the gearbox, clutch and driveshafts) and is typically replaced once during a vehicle's lifespan [10,11]. Grease is required for the lubrication of other vehicles parts such as bearings, seals and joints that cannot be lubricated by oils [12]. While EVs continue to require grease and transmission fluid, they no longer require engine oil due to the replacement of the engine with a battery as the source of power. EVs' lack of engine oil could represent significant losses in revenue for the conventional lubricants market, however, the requirement for battery cooling fluids represents a new opportunity for the industry [10]. This makes research and development of EV fluids a priority for businesses aiming to break into this new segment of the market.

Analogous to the fluids required for ICE vehicles, there are three distinct categories of EV fluids: e-transmission fluids, e-greases and e-thermal fluids. The 'e' prefix distinguishes these fluids from their conventional ICE vehicle counterparts, as EV fluids have a particular set of requirements for compatibility with EV components and materials. Firstly, e-fluids must be chemically compatible with new materials used in electric motors, lithium-ion batteries and electrical insulation. This includes new lightweight materials, such as polycarbonate plastics and carbon-fibre composites that are continually introduced to EV designs to improve range performance and, therefore, e-fluids must be highly inert [10,13]. Secondly, e-fluids must be electrically compatible to operate under high voltages and so require extremely low conductivity to sufficiently insulate the electronic components to prevent short circuits or electric shocks [10,14]. Thirdly, e-fluids must be magnetically compatible as certain electric motor designs utilise strong magnetic fields which could impact the flow of fluids and wear debris through the drivetrain [10].

2.2 EV Battery Cooling Systems

Lithium-ion batteries (LIBs) are the leading battery technology used in almost all EVs due to their high energy density and reliable operation. The optimal temperature range for LIB operation is 15-35°C, which provides optimal conditions for electrochemical reaction and ion transport [8]. At low temperatures the discharge capacity of LIBs is reduced significantly due to increasing electrolyte viscosity and greater internal resistance, whereas, at high temperatures LIBs can be damaged by electrode breakdown, electrolyte oxidation and membrane decomposition [15,16]. During charge and discharge cycles, heat can be produced by the electrochemical reaction, charge transfer and ohmic heating – therefore, a cooling system is required to maintain optimal battery temperature [17]. Various configurations of cooling system exist and are discussed below.

2.2.1 Direct Air Cooling

Air cooling is the simplest battery cooling configuration and is commonly utilised due to the ease of implementation. Air cooling has been effectively implemented since the early stages of EV development, such as in the 2010 Nissan Leaf, and continues to be used in some current EV models [18]. An air-cooling system works on the basic principle of air convection through the battery module to remove heat. Forced air convection can be achieved by active measures, such as an air compressor or fan, or passive systems utilise natural air convection [19]. While air cooling reduces system complexity and cost, this configuration places a significant limitation on the effectiveness of heat removal due to air’s low heat capacity and poor thermal conductivity. This makes air cooling unsuitable for applications with high discharge rates or warmer climates and, therefore, liquid cooling must be implemented to achieve more effective heat transfer.

2.2.2 Indirect Liquid Cooling

Indirect liquid cooling typically implements an aluminium cooling jacket or cooling plate that is in contact with the battery module [20]. The most commonly used coolant liquid is a water/glycol mixture which is pumped through channels in the jacket or plate to indirectly absorb excess heat from the battery. Indirect liquid cooling systems have been successfully implemented in many commercially available EVs, such as the Tesla Model S, and typically allow for higher performance systems than air cooling due to improved heat transfer [20,21]. Due to the high heat capacity and low viscosity of the water/glycol coolant, energy requirements for pumping are reduced when compared to air compression [19]. However, indirect liquid cooling systems do have drawbacks. Since cooling is only on the surface of the cooling jacket or shell, temperature distribution throughout the battery cells is inhomogeneous. The system also contributes a significant weight addition to the vehicle due to the aluminium cooling jacket or plate, ultimately reducing the drive range. The aluminium shell also limits the efficiency of heat removal due to the conduction of heat through the walls of the jacket. Furthermore, coolant leakage is a concern for battery short-circuit and the hazardous nature of glycol [19,20].

2.2.3 Direct Liquid (Immersion) Cooling

Direct liquid cooling, also termed 'immersion cooling', involves the use of a dielectric coolant that directly flows through the battery cells and physically contacts the battery electronics. The coolant is circulated with a pump through the battery module and then flows to a heat exchanger to release the absorbed heat to the environment before being recirculated [8]. This configuration presents many benefits over air cooling and indirect liquid cooling. The coolant liquid directly contacts the battery cells, maximising heat transfer efficiency and helping to maintain homogeneous battery temperature. Furthermore, the direct cooling configuration eliminates the need for fans or cooling jackets, reducing system complexity and weight. Despite promising advantages, immersion cooling is yet to be implemented in commercially available EVs due to various technological challenges including electrochemical corrosion, material compatibility and high viscosity of dielectric coolants [19,22].

2.2.4 Direct Phase Change Material Cooling

This configuration attempts to utilise the high latent energy required for phase change to passively remove heat from the battery. The battery pack is surrounded by a phase change material (PCM), typically a solid with a low melting point such as paraffin [23]. As the battery generates heat, this will be transferred to the PCM that will gradually reach its melting point, changing to the liquid state and absorbing a large amount of energy equivalent to the latent heat of fusion – rapidly cooling the battery. Similar configurations have also been designed to implement liquid to gas PCM, such as hydrofluoroether [19]. While the concept of these configurations is promising, allowing fully passive cooling with the removal of fans, pumps or moving parts, there are some key barriers to their implementation [24]. The primary difficulty lies in the complexity of volume expansion and two-phase flow during phase change, further hindered by the complicated mechanism for cooling and recycling the PCM to its original state after phase change [19,23]. Due to these challenges, cooling system with

PCMs have not been implemented in any commercially available EVs and further development of these systems is required to make them feasible for commercialisation.

2.2.5 Thermal Runaway

The implementation of an effective battery thermal management system not only has implications for vehicle performance but also plays a critical role in vehicle safety. Insufficient cooling that allows elevated and non-homogeneous battery temperatures can lead to thermal runaway, a serious safety concern for LIBs in EVs. Thermal runaway is caused by a series of chain reactions that can be initiated by overheating of battery cells [25]. These side reactions produce heat, further exacerbating the problem and leading to self-sustaining exothermic runaway reactions that can lead to extremely high temperatures resulting in battery fires and even explosions. Furthermore, propagation of the heat from the thermal runaway of a single cell to adjacent cells can rapidly lead to catastrophic incidents [25,26].

Immersion cooling systems offer more robust protection against thermal runaway than indirect liquid cooling and air cooling. The improved heat transfer and immersion of all battery cells in the coolant helps to control temperature spikes, establishing temperature uniformity throughout the battery pack and reducing the likelihood of hotspots forming in isolated cells [24]. Therefore, the development of effective dielectric coolants with optimal heat removal properties is not only important for performance but also, crucially, for safety improvement.

2.3 E-thermal Fluids

As the focus of this investigation will be the properties of base oils for e-thermal fluids, this specific branch of e-fluids is discussed below in further detail. E-thermal fluids are designed for use as the dielectric coolants in immersion cooling systems, where the fluid is in direct contact with battery cells and electronic components. Therefore, there are many properties of e-thermal fluids that are necessary for safe and optimal cooling performance. Furthermore, the intention is for e-thermal fluids to be 'fill for life', suggesting that they will be in operation for 10-20 years and they must possess long-term resistance to both electrical and thermal degradation.

2.3.1 Ideal Characteristics

As discussed previously, e-thermal fluids must fulfil the general characteristics required of e-fluids: electrical compatibility, thermal compatibility and chemical compatibility. Since e-thermal fluids will be in direct contact with battery cells and electronics, the fluid must be dielectric. A dielectric fluid is electrically non-conductive with high resistivity to act as an insulator to prevent battery short-circuiting [27]. The quality of a dielectric fluid can also be characterised by the dielectric dissipation factor, which indicates electrical energy losses to the fluid due to the presence of polar contaminants such as water or oxidation products [28]. It is desirable for dielectric fluids to have a low dissipation factor, as this means less electrical energy is lost as dissipated heat within the fluid. Therefore, e-thermal fluids must be highly resistant to oxidation caused by thermal or electrical degradation, as oxidation products will reduce the performance of the fluid and lead to energy losses within the battery modules.

Beyond the electrical characteristics of the fluid, the main function of the e-thermal fluid is to effectively remove excess heat from the battery. Therefore, the fluid's thermal and physical properties must be optimised to ensure effective fluid flow and heat transfer. A combination of high thermal conductivity, high specific heat capacity and low viscosity is desirable to achieve the most effective heat transfer [29]. Furthermore, low viscosity helps to reduce pumping energy requirements and promotes turbulent flow through the battery modules which further enhances heat transfer. Beyond the fluid characteristics, the cooling system design is also a crucial factor in determining the fluid flow regime which must be considered to achieve optimal heat transfer.

Another critical characteristic of e-thermal fluids is their compatibility with the copper components found in the battery and electric motor coils. In high voltage environments, electrochemical corrosion of copper is more likely and e-thermal fluids should be designed with protection against corrosion [14]. Copper compatibility can be tested using a standardised copper wire corrosion test following the ASTM D130 standards. Additive packages can be added to base oils for e-thermal fluids to inhibit the mechanisms of copper corrosion [10].

2.3.2 Integrated Lubrication & Thermal Management

Optimisation of electric vehicle design and reducing the weight of components helps to improve their performance and range. One proposal is to adopt an integrated drive-unit design, where a single e-fluid is used for cooling and lubrication of the electric drivetrain [30]. This would effectively combine the roles of e-thermal and e-transmission fluids into a single fluid that cools the battery and electric motor while also lubricating the moving parts in gearbox and driveshaft. This integrated design would allow for weight reduction by requiring only a single pump, ducting system and enclosure. Challenges exist with this combined approach, such as the simultaneous thermal management of both the battery and the motor adding extra cooling duty to the e-fluid [31]. However, with development the integrated design offers significant benefits for EV design efficiency and performance. Therefore, when considering the performance of e-thermal fluids it is also pertinent to consider their potential use as a lubricant in an integrated system.

2.3.3 Suitable Base Oils

Base oils for e-thermal fluid applications can be separated into two main categories: mineral oils and synthetic oils. Base oils are categorised into five groups by the American Petroleum Institute (API), with Groups I, II and III representing mineral oils while Groups IV and V generally represent synthetic oils [32]. In terms of mineral oils, Group III are the most suitable due to their higher viscosity index and lower sulfur content – making their chemical and physical properties more stable for e-thermal fluid applications.

When considering synthetic oils, Group IV base oils include polyalphaolefins (PAOs) that would be suitable for e-thermal fluid applications due to good stability under extreme conditions and high viscosity index. However, the synthesis process for producing PAOs currently has limited capacity potentially restricting their application due to the cost and material availability [33]. Finally, Group V base oils include all other synthetic oils. Particularly promising candidates for e-thermal fluid applications are ester-based oils such as diesters and polyolesters, as these fluids possess good dielectric properties, effective low temperature performance and promising thermal properties [34,35].

2.4 State of the Art

Due to the relative novelty of EV fluids, the body of work in literature that analyses their characteristics and performance is limited. There are a small number of commercially available e-thermal fluids, but their formulation and characteristics are often highly confidential. These include 'AmpCool' by Engineered Fluids, 'Novec' by 3M, 'Galden' by Solvay and 'MIVOLT' by M&I Materials [36-39]. Furthermore, some of the leading global lubricant manufacturers, such as Shell and ExxonMobil, have invested into the development of EV-fluids demonstrating a clear shift in the market [14,40]. As commercial development of e-fluids has gained momentum in recent years, the number of academic studies in literature has also seen a notable increase. However, many of these analyse the performance of immersion cooling system without discussing or justifying the choice of e-thermal fluid, and only a select few compare base oils for e-thermal fluid applications.

Jithin and Rajesh set up a numerical model of a LIB direct liquid cooling system, and compared the cooling performance of three dielectric coolants: deionised water, mineral oil and an engineered synthetic fluid (AmpCool) [41]. Their findings clearly show that deionised water is the more effective coolant due to its high thermal conductivity and heat capacity, and the synthetic oil shows marginally better cooling performance than the mineral oil. Despite these findings, it should be noted that deionised water possesses poor tribological properties for applications as a lubricant and therefore could not be applied in an integrated drive-unit design. Therefore, deionised water is not considered in this work, however, its properties of high thermal conductivity, high heat capacity and low viscosity provide a good benchmark for suitable oils to be compared to.

Hurley *et al.* performed a series of measurements to characterise base oil's electrical, thermal and physical properties for electric drivetrain applications [42]. Their study assessed various base oils, including GIII mineral oils and synthetic oils, and compared their cooling performance based on the Mouromtseff number. Their results generally conclude that certain synthetic esters show better cooling performance than mineral oils and PAOs. It is suggested that esters with higher molecular weight and longer molecular chains have superior thermal properties due to intramolecular thermal conduction. The study also investigated the impact that additive packages had on the base oil properties, and it was found that finished fluids had lowered viscosity and increased electrical conductivity. When considering the results of the current study, it is important to be aware of the impact that additives may have on the base oil properties presented within this report.

An investigation into the effects of oxidative aging on the cooling performance of EV fluids was carried out by Rivera *et al.* [43]. They tested three fully formulated oils, one with a blend of GI base oils and the others with blends of GIII base oils. Aging of the fluids was performed at 150°C and 170°C with forced air flow for 168 hours and 216 hours. Their results demonstrate that the GI formulated oil was most sensitive to property changes after aging that negatively affected the cooling performance, such as increasing viscosity and decreasing heat capacity. They conclude that GIII formulated oils would be more suitable for EV fluid applications due to more stable properties after again demonstrating a superior oxidation resistance when compared to the GI oil.

This investigation aims to fill a gap in the current state of the art by studying the effects of both electrical and thermal degradation on a range of the most suitable base oil types for e-thermal fluid applications. While limited research exists, the studies generally investigate pre-formulated fluids without justifying the base oil selection. Certain studies have investigated the properties of selected fresh base oils but do not consider the oxidative aging caused by thermal or electrical degradation. Furthermore, a wider range of research may exist for other applications, such as insulation oil for electrical transformers, but research that specifically focusses on EV fluid applications remains limited. Therefore, this research builds upon previous literature while focussing on the niche of electrical and thermal degradation that is uncommon in the state of the art.

3 Methodology

3.1 Electrical Degradation

Electrical degradation of the base oils was performed using the 'Huazheng HZJQ-X1 Transformer Oil BDV Tester'. The equipment is comprised of a small oil cup containing hemispherical electrodes submerged in the oil sample and operates at room temperature. The electrodes are conventionally separated by a gap width of 2 mm, in line with ASTM D149 standard for breakdown voltage (BDV) testing. The voltage applied through the electrodes is gradually increased at a rate of 5 kV/s until charge is carried through the oil between the electrodes, producing a breakdown discharge. To electrically degrade the base oils, 1000 breakdown discharges were performed. The real-world electrical degradation that e-thermal fluids will experience in immersion cooling applications is largely unknown, and therefore this method was developed to achieve accelerated degradation for a 'worst case scenario' of the degradation that may occur during the operating lifespan of these fluids.

3.2 Thermal Degradation

The oils were subject to accelerated thermal aging to attempt to simulate the degradation that may occur across the operating lifetime of an e-thermal fluid. Approximately 500 mL of the fresh oil samples were transferred into a large conical flask and a pure copper strip placed into the flask with the sample. The purpose of the copper is to act as a form of catalyst to accelerate the thermal aging effects, promoting oxidation of the oil sample to emulate what may happen during years of operation in a vehicle. The conical flask, with oil sample and copper strip, was then placed in the thermal bath set to 150°C for 120 hours. The thermal aging method was adapted from the ASTM D130 standard, which assesses corrosiveness of petroleum products to copper. Once removed from the thermal bath, the samples were allowed to cool to room temperature before being transferred to air-tight containers to prevent absorption of water from humidity in the air.

3.3 Breakdown Voltage

The breakdown voltage of the samples was determined using the 'Huazheng HZJQ-X1 Transformer Oil BDV Tester'. The BDV was determined for fresh, electrically degraded and thermally degraded samples of each of the base oils. The equipment was set to perform the BDV tests according to the ASTM D149 standard. This standard requires hemispherical electrodes to be separated by a gap of 2 mm. Once the sample was loaded into the oil cup, a magnetic bead stirrer was used to mix the sample for two minutes before the first test was initiated and the stirrer continued throughout testing to ensure homogeneity of the sample. The voltage was steadily increased at a rate of 2 kV/s until a breakdown discharge was detected. A total of five measurements were taken for each sample, with a wait time of 2 minutes between each breakdown test. Throughout testing, the oil samples were maintained at room temperature, between 15-25°C, in accordance with the ASTM D149 standard.

3.4 Resistivity & Dissipation Factor

Oil resistivity and dissipation factor were measured using the DF9010 system manufactured by APT Power Technology Co. The equipment was set to perform measurements in accordance with the IEC 60247 standard. The oil sample cup is filled with 90 mL of the oil, which fills a small test cell. The small test cell was filled and drained three times with the sample to clean the equipment by displacement of any previous residual oil. The test procedure was then initiated, with the sample heated to 90°C and measurements taken automatically by the equipment. The equipment generates a DC voltage and measures the current through the test circuit to calculate the resistance and resistivity of the sample. Five to eight readings were taken for each oil sample, depending on concordance of results.

3.5 Thermal Properties

Measurement of thermal conductivity and heat capacity were performed using the Thermtest THW-L1 system. This equipment uses the transient hot wire (THW) method to directly measure thermal properties of liquids, following the ASTM D7896-19 standard. The measuring instrument utilises a thin platinum wire that is submerged in a measuring cell containing approximately 20 mL of the oil sample. Before testing, the instrument was calibrated using distilled water at 20°C to ensure accuracy of the results. The sample cell was then prepared with the oil for testing, inserted into the temperature controller and a schedule of measurements setup in the Thermtest software. For each sample, the schedule was set to take measurements at 10°C intervals from 20°C to 120°C. At each temperature step three readings were recorded, with a 10-minute delay between tests to ensure isothermal conditions are maintained.

3.6 Viscosity & Density

Viscosity and density of the samples were measured using the Anton Paar SVM 3001 Viscometer, which conforms to the ASTM D7042 standard. Readings of kinematic viscosity, dynamic viscosity and density were recorded at 10°C intervals from 20°C to 120°C. The sample to be tested was prepared in a 20 mL syringe. To begin testing, the temperature was set to 20°C and approximately 1.5 mL of the sample injected into the inlet nozzle to fill the sample cell. When prompted by the equipment, a further 1 mL of the sample was injected prior to the reading at each temperature step to refill the sample cell. Between the testing of different oil samples, the equipment was cleaned by injection of 10 mL of toluene and 10 mL of methanol and dried using compressed air to ensure there was no cross contamination that may interfere with the measurements.

3.7 Water Content

The water content of the oil samples was measured to parts per million (ppm) accuracy by implementing the Karl Fischer Coulometric (KFC) titration method using the Metrohm 917 Coulometer equipment. The KFC method involves the consumption of water contained in the sample by reaction with iodine. Pure iodine reagent is produced electrochemically by the equipment for high-precision dosing. The endpoint of the titration is detected voltametrically by applying a current between two platinum electrodes. When a trace amount of unreacted iodine is present in the solution, the voltage difference between the platinum wires drops significantly and signals that all of the water has been consumed by the reaction. Readings were repeated until three concordant results within ±10% were obtained.

3.8 Fourier-Transform Infrared Spectroscopy

FTIR spectroscopy was performed using the A2 Technologies spectrometer, with the iPAL instrument attachment for dedicated oil and lubricant sampling. The equipment measures in the spectral range from 4000 to 650 cm^{-1}. The results of the spectroscopy were analysed qualitatively, identifying signature peaks that are associated with specific functional groups and chemical structures. Key changes in the spectrums before and after degradation were identified as key areas of interest, showing chemical changes such as oxidation that could then be related to changes in the physical, thermal and electrical properties.

3.9 Uncertainties

Most of the equipment used for gathering results has an associated measurement uncertainty (σ_{equip}) reported by the manufacturer as a result of the inherent accuracy of the instrumentation. Where available, the equipment uncertainty is stated for each piece of equipment in Table 1, below:

Table 1: Measurement uncertainties reported by equipment manufacturers.

Equipment	Measured Parameter	Unit of Measurement	Measurement Uncertainty
Huazheng HZJQ-X1 Transformer Oil BDV Tester	Breakdown Voltage	kV	± (reading × 3%)
DF9010 Oil DF&R System	Resistivity	GΩm	± (reading × 10%)
	Dissipation Factor	%	± (reading × 1% + 0.001)
Metrohm 917 Coulometer	Water Content	ppm	± 3 ppm

Where repeated measurements have been taken and averaged there is also an associated statistical uncertainty, often reported as the standard error (σ_{SE}), which is calculated as follows:

$$\sigma_{SE} = \frac{S}{\sqrt{N}} \tag{1}$$

Where S is the standard deviation of the measurements and N is the number of measurements recorded. The standard error reflects the uncertainty that arises from variability of a repeated measurement. Assuming that the standard error and equipment uncertainty are independent and uncorrelated, they can be combined into a single uncertainty value as follows:

$$\sigma_{total} = \sqrt{\sigma_{equip}^2 + \sigma_{SE}^2} \tag{2}$$

Equation 2 combines the uncertainties according to the general principles of error propagation. Where both repeated measurements were obtained and the equipment uncertainty is known, the total uncertainty is reported in the results. If only a single reading was taken, only the equipment uncertainty is reported and where the equipment uncertainty is unknown only the standard error is reported. A sample calculation for the determination of uncertainties is shown in Appendix A. Furthermore, the raw data for repeated results from which the uncertainties were calculated can be found in Appendix B.

4 Results & Discussion

4.1 Fourier-Transform Infrared (FTIR) Spectroscopy

It is pertinent to open the discussion of the results with the findings of the FTIR spectroscopy, as these results serve as an underlying basis to understanding and explaining the effect degradation has on the physical, electrical and thermal properties of the oils.

4.1.1 Group III

Figure 1, below, shows the absorption spectrums for the fresh, thermally aged and electrically aged GIII oil:

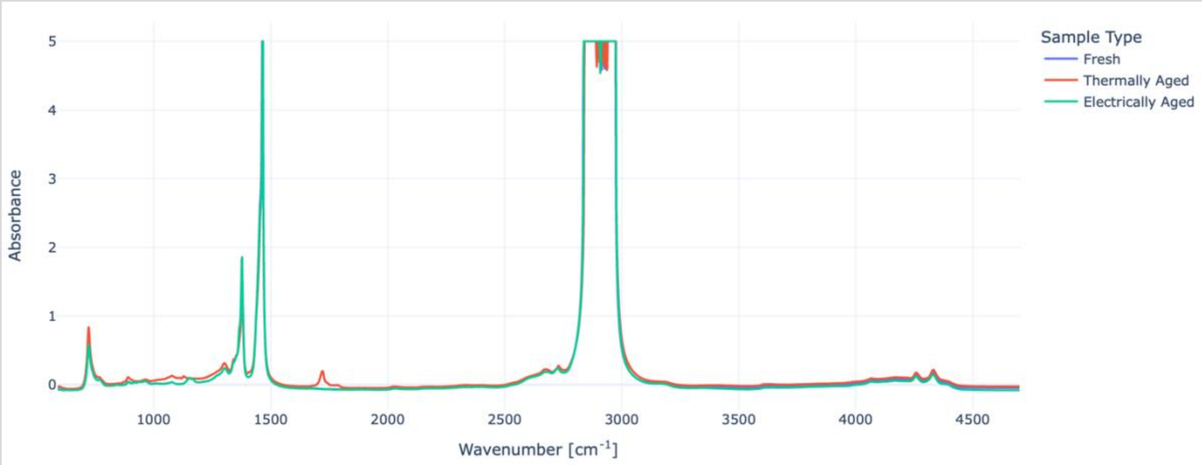

Figure 1: FTIR absorbance spectrum for GIII oil samples.

As can be observed, the spectrum of the fresh oil sample is almost fully overlaid by the thermally degraded and electrically degraded spectrums, however, small changes to the spectrum give an important insight into the changes to chemical structure that have occurred due to the degradation processes. The base spectrum is composed of four main peaks, characterising the basic hydrocarbon structure of the GIII oil. The first peak at ~720 cm^{-1} represents the presence of unsaturated hydrocarbon chains, with trans double bonds such as R–CH=CH–R or $R_2C=CH_2$. The relatively small absorbance at this wavelength suggests the GIII oil is largely composed of saturated hydrocarbon chains. The next two peaks at ~1380 cm^{-1} and ~1470 cm^{-1} represent the bending C–H bonds within CH, CH_2 and CH_3 groups. The absorption wavelengths of these different C–H bonds coincide, resulting in high absorbance and the narrow peaks characterise the oil's non-polar nature. The final large peak between 2830 cm^{-1} and 2975 cm^{-1} represents the stretching C–H bonds within CH, CH_2, CH_3 and aromatic groups and similarly indicates the largely saturated hydrocarbon composition of the GIII oil.

The most prominent points of difference are shown between the fresh and thermally degraded spectrums, with the degraded oil sample showing slightly higher absorbance in the 700-1300 cm^{-1} region as well as showing a small additional peak at ~1720 cm^{-1}. The high absorbance at lower wavenumbers suggests a greater level of unsaturation in the thermally aged sample. This is likely due to the cracking of saturated hydrocarbon chains at the high temperature, causing a loss of hydrogen and the formation of shorter unsaturated chains within the oil. The small absorbance peak at ~1720 cm^{-1} is likely due to stretching C=O bonds, which suggests the oil has experienced a small amount of oxidation during thermal degradation. The greater level of unsaturation as well as the increased polarity caused by the presence of the carbonyl groups can affect the inter- and intra-molecular interactions which can change the oil's physical, thermal and electrical properties. This will be discussed further in the following sections. In terms of the electrically degraded oil sample, this presents no changes in the spectrum from the fresh sample and therefore it can be assumed that the electrical degradation process did not drastically alter the chemical structure of the oil.

4.1.2 PAO

The absorbance spectrum for the each of the PAO oil samples is shown in Figure 2, below:

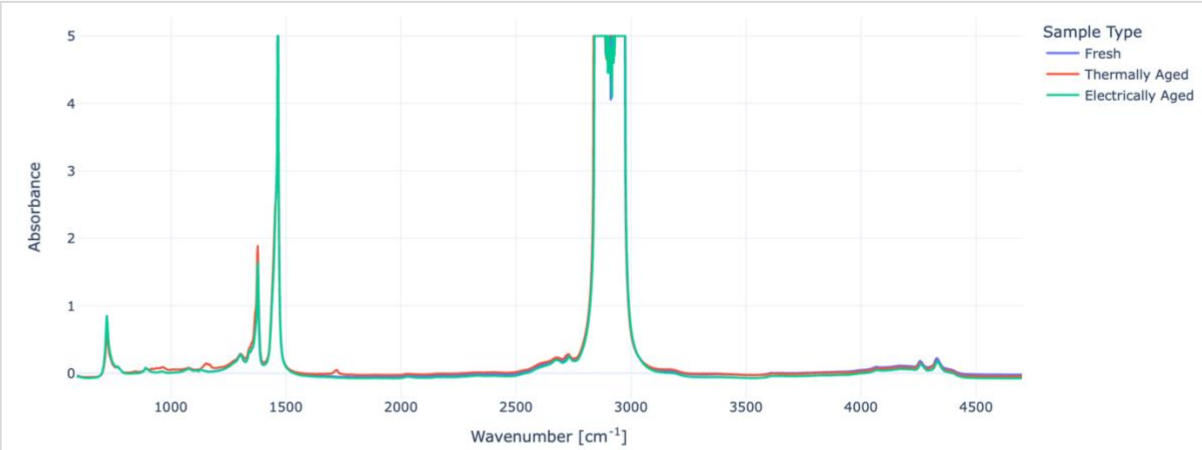

Figure 2: FTIR absorbance spectrum for PAO oil samples.

The PAO spectrum is very similar to the GIII spectrum, indicating their structural similarities. The four main peaks are, again, observed indicating the presence of saturated and unsaturated hydrocarbon bonds. Like the GIII oil, electrical degradation appears to have had very little effect on the chemical structure of the PAO, however, there are some notable effects of the thermal degradation. The small peak at ~1720 cm^{-1} presents itself again, likely indicating a small amount of oxidation and the formation of C=O bonds. Crucially, it should be noted that the absorbance shown at this wavelength is smaller than that of the thermally aged GIII, indicating that the PAO may have higher oxidation resistance. The thermally degraded PAO also shows another small absorption peak at ~1160 cm^{-1} which may also be indicative of oxidation in the form of a C–O stretching bond. Absorption in the 700-1300 cm^{-1} region suggests the possibility of hydrocarbon cracking and desaturation, similar to that shown in the GIII spectrum.

4.1.3 Diester

Shown in Figure 3, below, is the absorbance spectrum for the diester oil:

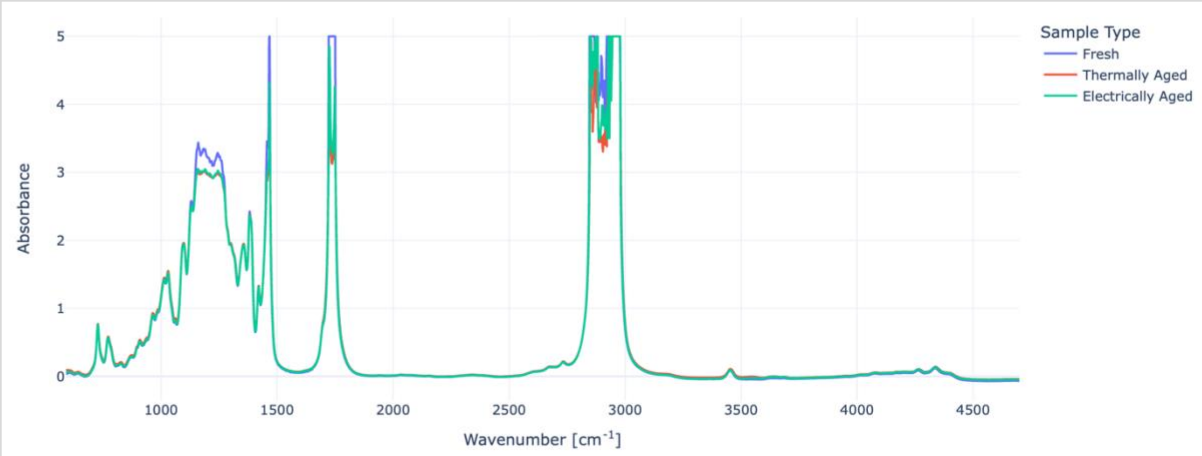

Figure 3: FTIR absorbance spectrum for diester oil samples.

It can be observed that the spectrum of the diester is significantly different from the GIII and PAO oils, due to the natural presence of oxygen in its structure. The structure of esters is characterised by the 'ester link' which is shown diagrammatically in Figure 4, below:

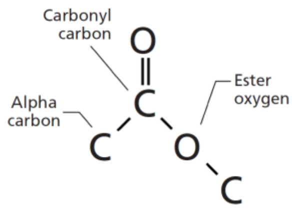

Figure 4: Chemical structure of an ester link functional group [44].

This chemical structure has a very clear signature shown in the absorbance peaks, known as the 'rule of three' [44]. The stretch of the C=O bond is shown in the peak at 1720-1755 cm^{-1} indicating the presence of the carbonyl group within the ester link structure. The stretch of the C–O bond from the carbonyl carbon to the ester oxygen is characterised by absorption in the 1160-1210 cm^{-1} region while the C–O stretch from the ester oxygen to the opposite carbon is shown by absorption in the 1030-1100 cm^{-1} region. The absorption from both of these C–O stretching bonds contributes to the formation of the wide peak in the general region of 1000-1250 cm^{-1}. The peaks at ~1470 cm^{-1} and 2830-2975 cm^{-1}, also shown in the GIII and PAO spectrums, represents the C–H bending and C–H stretching bonds in the hydrocarbon chain sections of the ester structure.

The spectrums for the thermally and electrically degraded diester oil samples both show changes from the fresh sample. There is a notable drop in absorption in the 1150-1250 cm^{-1} and 1720-1755 cm^{-1} regions, suggesting a lower concentration of ester linkages within the oil structure. It can be proposed that during the degradation processes the diester is undergoing a hydrolysis reaction with absorbed water, whereby the ester links are broken into their constituent alcohol and carboxylic acid molecules. This is further discussed under the water content results to follow. There is also a lower absorption in the peak at ~1470 cm^{-1} suggesting a lower concentration of C–H bonds and, therefore, greater desaturation within the ester structure.

4.1.4 Polyolester

Figure 5, below, shows the absorbance spectrum for the polyolester oil:

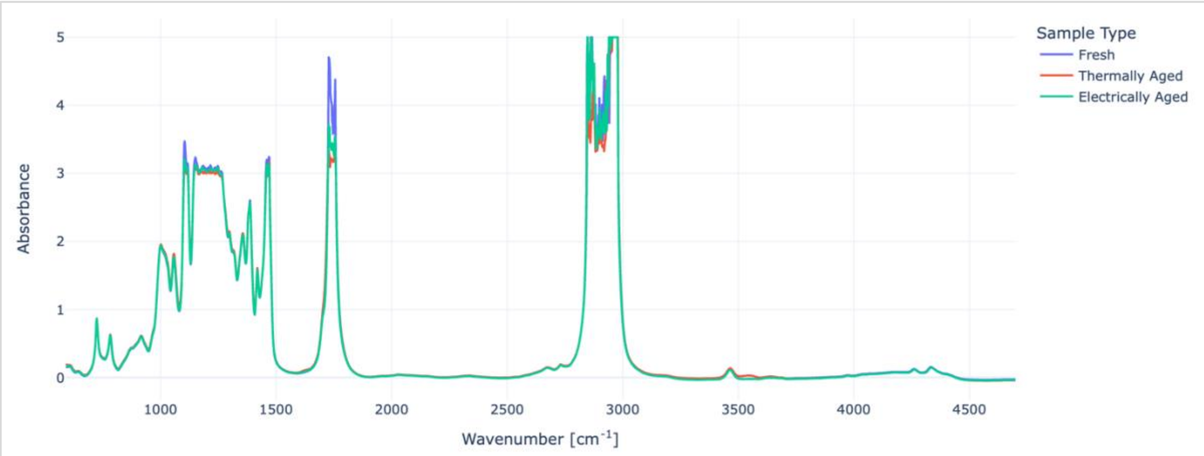

Figure 5: FTIR absorbance spectrum for polyolester oil samples.

The spectrum shows the same features as discussed above for the diester, with the distinctive 'rule of three' signature of the ester link shown again. The electrical and thermal degradation of the polyolester show a similar trend to the diester, with a decrease in absorption in the 1150-1250 cm^{-1} and 1720-1755 cm^{-1} regions, but generally it is decreased to a lesser extent than the diester. This suggests the polyolester may be slightly more resistant to degradation by thermal and electrical stresses than the diester. Similar to the diester, the lower absorption at the signature peaks of the ester link could suggest hydrolysis of the polyolester molecules, however, the lesser decrease in absorbance suggests hydrolysis occurred to a lesser extent in the polyolester.

4.2 Water Content

The water content of the oil plays a crucial role in its electrical properties, as even a very slight increase in the concentration of water present can greatly decrease the oil's resistivity. Therefore, the change in water content under degradation is important to consider, as this will have implications for the oil's continued capacity for high resistivity that is required by immersion cooling applications. Figure 6, below, compares the water content of each of the oils before and after degradation with associated error bars shown in red:

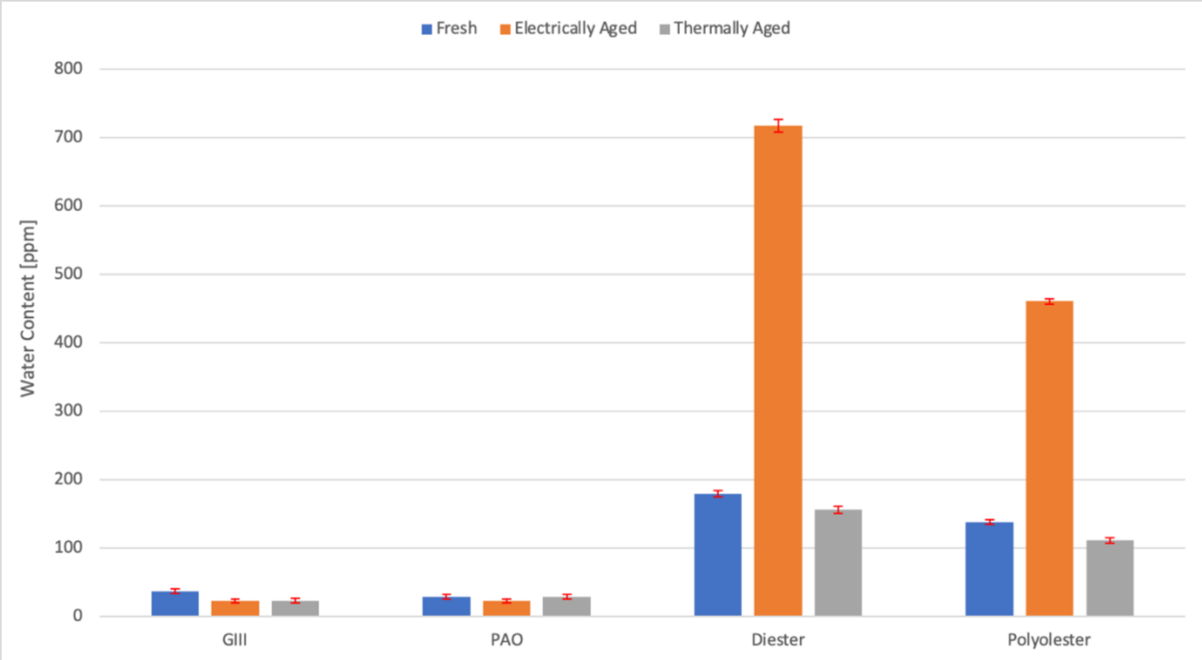

Figure 6: Water content of fresh and degraded oil samples.

The results above show a clear divide between the water content of the hydrocarbon-based oils and the ester-based oils, with the GIII and PAO showing low water content that is insignificantly changed by degradation and the esters showing higher water content that is changed significantly by electrical degradation. For the GIII and PAO, the water content slightly decreases after both electrical and thermal degradation. This can be simply explained as the evaporation of small amounts of water present in the oil, caused by the constant high temperature present during thermal degradation or the momentary high temperature present during an electrical breakdown spark. However, the increase in water content of the ester oils during electrical degradation is an unexpected phenomenon that requires further exploration.

It was previously hypothesised from the FTIR spectroscopy results that the presence of water within the ester oils could be causing a hydrolysis reaction during degradation, as a decrease in the absorbance peaks of C–O, C=O and C–H bonds suggests the breaking of the ester linkage groups. Despite the consumption of water by this reaction, the electrically degraded ester oils show a significant increase in water content. This is likely due to absorbance of water from the humidity in the air, which was in contact with the oil sample for 2-days during its degradation period in the breakdown voltage sample cup. Due to the polar nature of the ester oils, they have a high affinity for water absorption, especially in environments with high humidity. The thermally degraded ester oil samples show a slight decrease in water content, due to the high temperatures boiling off absorbed water.

4.3 Thermal & Physical Properties

4.3.1 Dynamic Viscosity

Generally, lower viscosity is desirable for e-thermal fluid applications, as this reduces pumping costs and improves heat transfer characteristics. The results of the viscosity testing for the fresh and degraded oil samples are shown in Figure 7 and the average percentage change of the viscosity after degradation is shown in Figure 8, below:

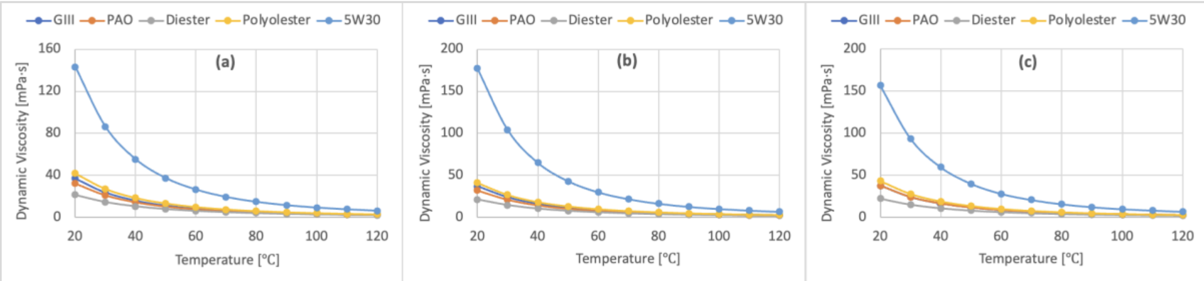

Figure 7: Dynamic viscosity vs. temperature for (a) fresh, (b) electrically degraded and (c) thermally degraded oils.

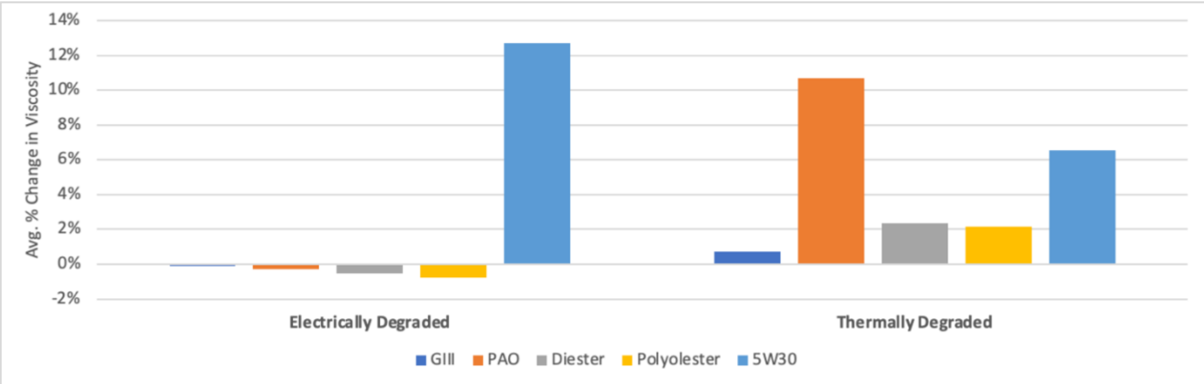

Figure 8: Average percentage change in dynamic viscosity after degradation compared to fresh properties.

As shown, the diester has the lowest viscosity within the temperature range of 20-50°C, which is the most typical operating range for an e-thermal fluid. The diester's viscosity also has the lowest temperature dependence and therefore remains relatively constant throughout the whole temperature range. This would suggest that in terms of viscosity, the diester would be most suitable for e-thermal fluid applications due to reduced pumping duty and high viscosity index. However, the GIII, PAO and polyolester show very similar trends in viscosity that are only marginally higher than the diester.

Figure 8 shows that electrical degradation had a very minimal effect on the viscosity of the base oils, however, thermal degradation resulted in a slight increase in viscosity for each of the oils. The most significant increase of over 10% was observed after thermal degradation of the PAO, likely due to the desaturation of the hydrocarbon chains shown in the FTIR spectrum leading to hydrocarbon molecules bending to a greater extent and increasing the internal friction. Increasing viscosity under thermal degradation is undesirable, as this can reduce heat transfer efficiency and increase pumping energy requirements.

When considering the 5W30 engine oil as a comparison, the suitability of the four base oils' viscosity is emphasised. The 5W30's viscosity changed significantly with changes in temperature and its viscosity at lower temperatures was also increased considerably by thermal and electrical degradation. This would not be preferable for e-thermal fluid applications, due to variability of viscosity affecting cooling performance at low temperatures as well as increasing the pumping requirements. However, the four base oils tested show significantly better viscosity properties that would be suitable for e-thermal fluid applications, with diester demonstrating the most optimal viscosity properties overall.

4.3.2 Density

For e-thermal fluid applications, higher density is preferable to achieve an improved capacity for heat removal as well as being beneficial for achieving turbulent flow which assists with more efficient heat transfer. The density readings for the fresh and degraded oil samples are shown in Figure 9, below, alongside the average percentage change in density shown in Figure 10:

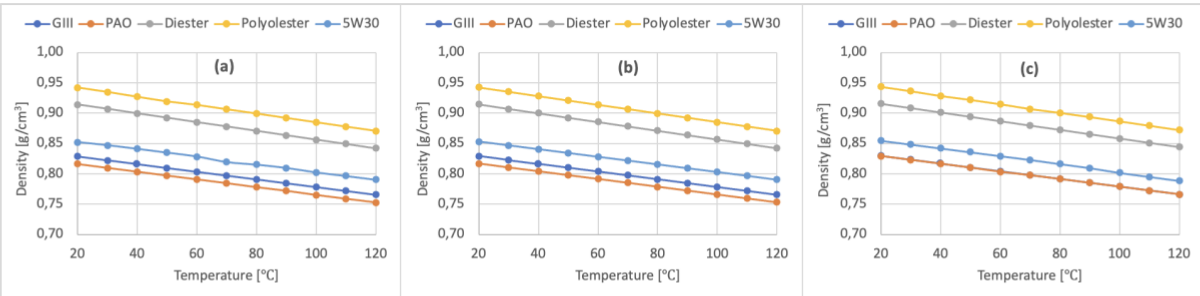

Figure 9: Density vs. temperature for (a) fresh, (b) electrically degraded and (c) thermally degraded oils.

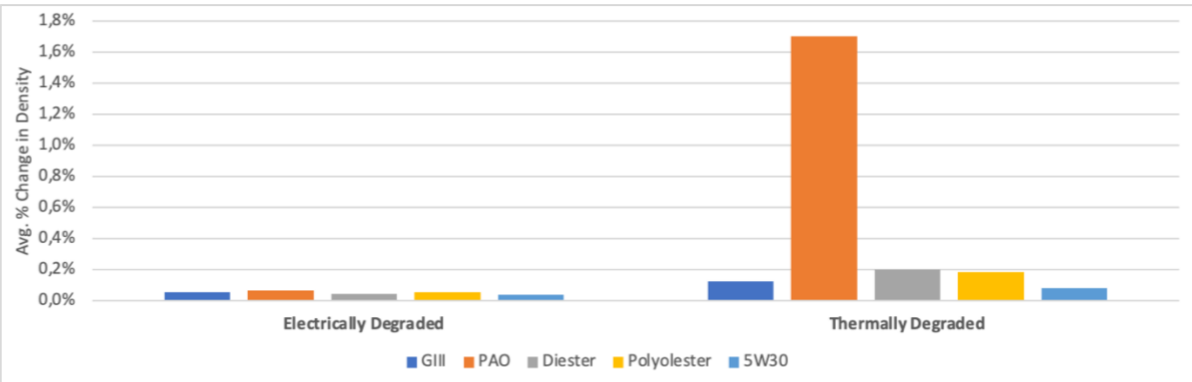

Figure 10: Average percentage change in density after degradation compared to fresh properties.

As shown in Figure 9, polyolester has the highest density closely followed by the diester, making these oils the most suitable in terms of density considerations. The PAO showed the lowest density and had the greatest increase in density following thermal degradation, likely due to the formation of shorter desaturated hydrocarbon chains that can achieve tighter molecular packing. This was the only significant impact of degradation on density, in all other cases this property remained relatively unchanged.

4.3.3 Thermal Conductivity

Thermal conductivity is one of the most critical properties of a heat transfer fluid, with higher thermal conductivity allowing for more effective removal of heat and efficient dispersion of heat for homogenised temperature control. Figures 11 and 12, below, show the recorded thermal conductivities of the oil samples and the average percentage change after degradation:

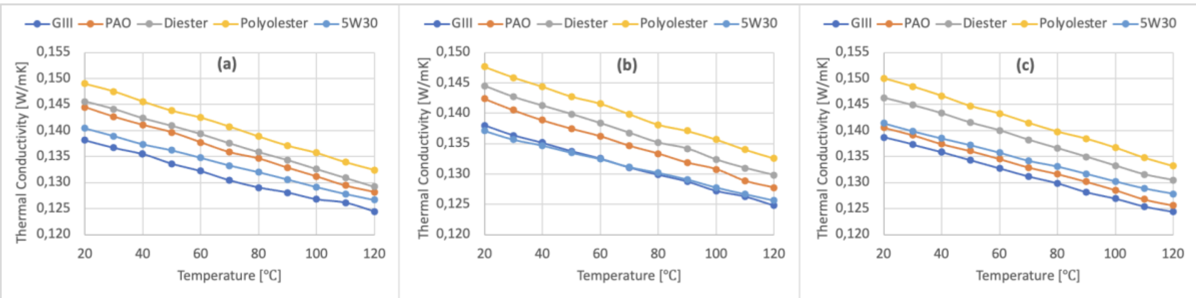

Figure 11: Thermal conductivity vs. temperature for (a) fresh, (b) electrically degraded and (c) thermally degraded oils.

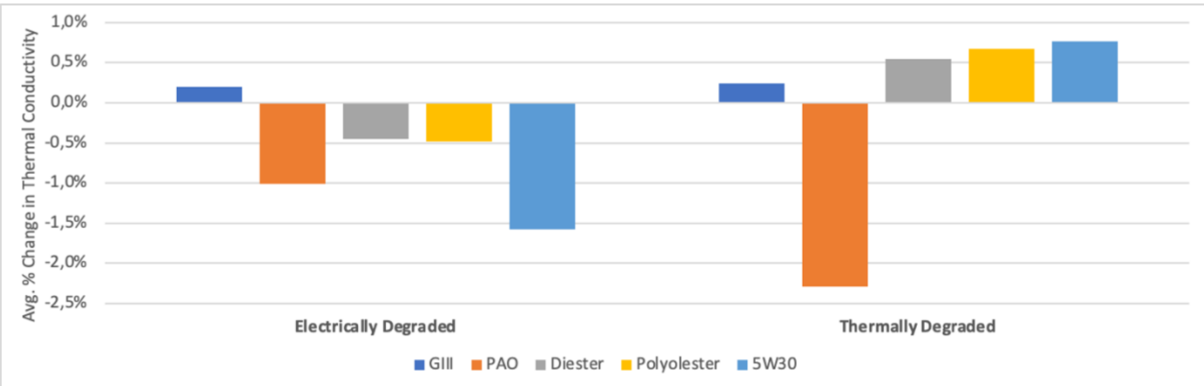

Figure 12: Average percentage change in thermal conductivity after degradation compared to fresh properties.

It can be observed that polyolester has the highest thermal conductivity in all cases and a general trend is shown that the synthetic oils have more effective heat transfer than the mineral oils. The thermal degradation slightly increased the thermal conductivity of the ester oils while significantly decreasing that of the PAO. This is likely a factor associated with the increase in the PAO's viscosity after thermal degradation leading to less efficient conduction of thermal energy. Conversely, the electrical degradation slightly decreased the thermal conductivity of all of the oils except for the GIII which was minimally changed.

4.3.4 Specific Heat Capacity

High specific heat capacity is required by e-thermal fluids to allow them to effectively remove excess heat without the fluid itself raising temperature excessively. The results of the specific heat capacity tests for each of the oil samples are shown in Figure 13, below, and the average percentage change after degradation is shown in Figure 14:

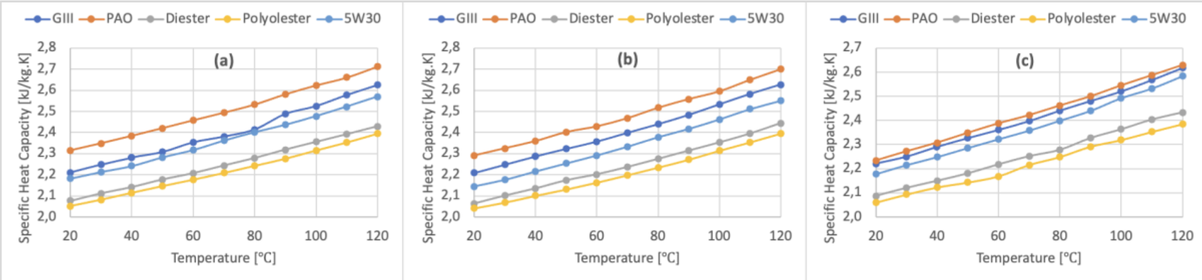

Figure 13: Specific heat capacity vs. temperature for (a) fresh, (b) electrically degraded and (c) thermally degraded oils.

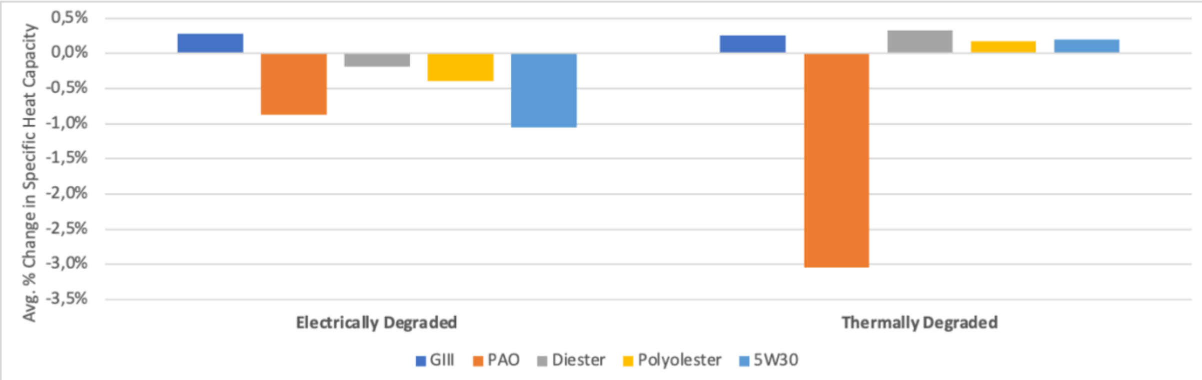

Figure 14: Average percentage change in specific heat capacity after degradation compared to fresh properties.

It can be observed that PAO has the highest specific heat capacity, but it is also the only oil in which the heat capacity decreased significantly under thermal degradation. With thermal degradation causing a greater degree of unsaturation in the PAO, the specific heat capacity is decreased due to a loss in vibrational degrees of freedom. Electrical degradation did not have a significant impact on the specific heat capacity of any of the oils. The ester oils, diester and polyolester, have the lowest specific heat capacity of all of the oils samples.

To propose which oil has the most effective thermal properties it is important to consider both thermal conductivity and specific heat capacity simultaneously. It can be observed that while PAO's thermal conductivity is slightly lower than that of the esters, the esters have a significantly lower specific heat capacity than PAO. Therefore, overall, it can be proposed that PAO possesses the most effective thermal properties for e-thermal fluid applications out of the four base oils tested. Despite this, it should be noted that PAO's thermal properties were more sensitive to thermal degradation than the other oils, which could perhaps be addressed with the addition of additives in the fully formulated oil, for example viscosity stabilisers.

4.3.5 Mouromtseff Number

While it can be proposed that PAO has the most effective thermal properties of the base oils tested, the effectiveness of heat transfer relies not only on thermal properties but on the physical properties of density and viscosity. High density and low viscosity are desirable for more effective heat transfer as well as for promoting turbulent flow which enhances convection of heat. The Mouromtseff number incorporates all of these parameters into a figure of merit for heat transfer fluids. The Mouromtseff number is calculated according to Equation 3, below, where the exponents are empirically derived for heat transfer under turbulent fluid flow:

$$Mo = \frac{\rho^{0.8}\lambda^{0.67}c_p^{0.33}}{\mu^{0.47}} \tag{3}$$

Where density (ρ), thermal conductivity (λ) and specific heat capacity (c_p) are on the numerator and dynamic viscosity (μ) is on the denominator.

The Mouromtseff numbers for each of the oil samples is shown below in Figure 15 and Figure 16 illustrates the percentage change in heat transfer merit after degradation:

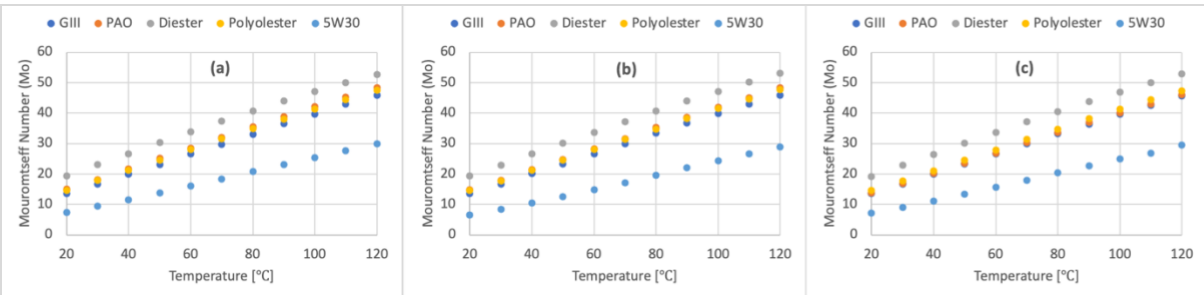

Figure 15: Mouromtseff number vs. temperature for (a) fresh, (b) electrically degraded and (c) thermally degraded oils.

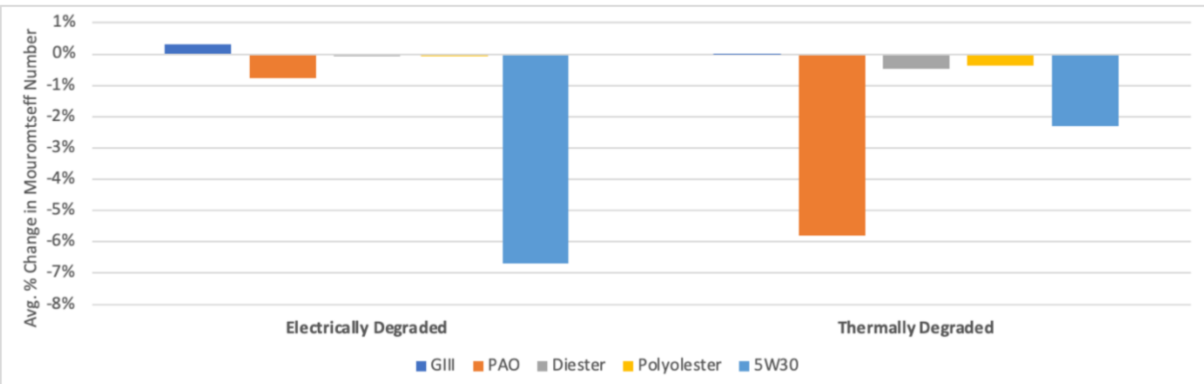

Figure 16: Average percentage change in Mouromtseff number after degradation compared to fresh properties.

As shown above, the diester has the highest Mouromtseff number indicating it has the most optimal properties for heat transfer overall. When compared to PAO, the diester's higher density and lower viscosity may make its heat transfer characteristics marginally better, however, all of the base oils tested show promising heat transfer merit as emphasised by the baseline of the 5W30 engine oil which has significantly lower Mouromtseff numbers mainly related with higher viscosity values.

4.4 Electrical Properties

4.4.1 Dissipation Factor

The dielectric dissipation factor is a measure of the inefficiency of the insulating properties of the dielectric fluid. It is the ratio of an insulating fluid's ohmic properties to its capacitive properties. An ideal dielectric fluid would have very low ohmic properties and high capacitive properties, meaning there is no conduction through the fluid and dissipation factor approaches zero. However, degradation of the dielectric fluid can lead to impurities and oxidation products which lead to the flow of current through the fluid and, therefore, losses to ohmic resistance. A higher dissipation factor is associated with higher dielectric losses, meaning electrical energy is lost to the insulating fluid. Figure 17, below, shows the results of the dissipation factor measurements for each of the oils samples:

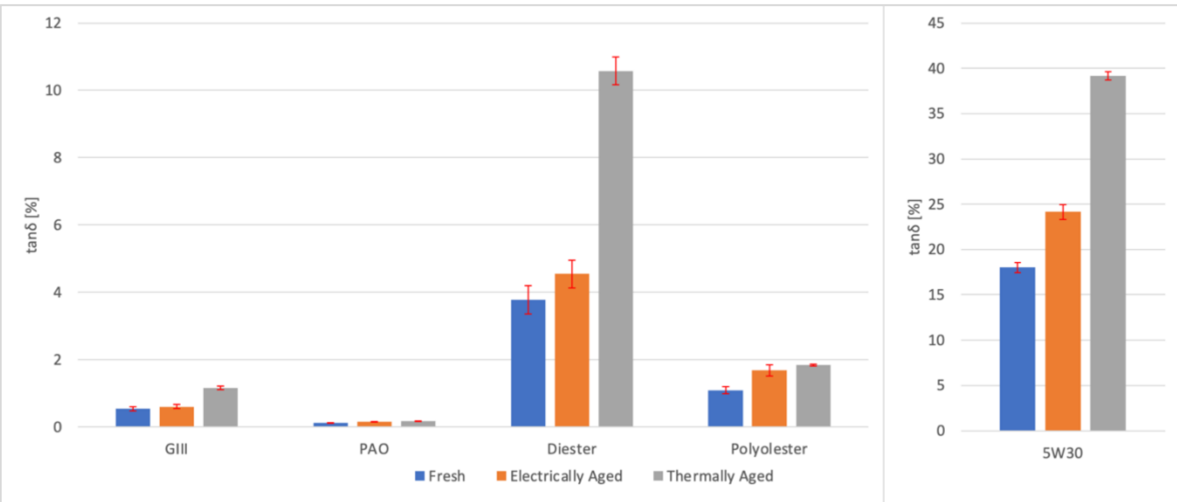

Figure 17: Dissipation factor (tanδ) of fresh and degraded oil samples.

The PAO oil has the lowest dissipation factor that is relatively unaffected by degradation, demonstrating the most effective insulating properties. The GIII mineral oil has the next lowest dissipation factor, however, it is slightly increased after thermal degradation due to the formation of oxidation products. The diester and polyolester show higher dissipation factor than the GIII, likely due to their polarity and higher water content. The 5W30 engine oil has significantly higher dissipation factor than the base oils due to the presence of additives, leading to great inefficiency of the fluid's insulating properties. The impact of degradation on the dissipation factor results are further discussed below alongside resistivity.

4.4.2 Resistivity

Resistivity is an inherent property of the oils and measures the electrical resistance of oil with given cross-sectional area and length. For e-thermal fluid applications, high resistivity and low dissipation factor are desirable to fully insulate the battery cells in immersion cooling systems. If the fluid's resistivity was too low, this increases the likelihood of electrical conduction through the fluid during high voltage applications which would lead to short circuiting of the battery. Resistivity is also closely related to the dissipation factor, shown in Figure 17 above, and generally as dissipation factor decreases resistivity will increase. Shown in Figure 18, below, are the results of the resistivity measurements for the fresh and degraded oils samples:

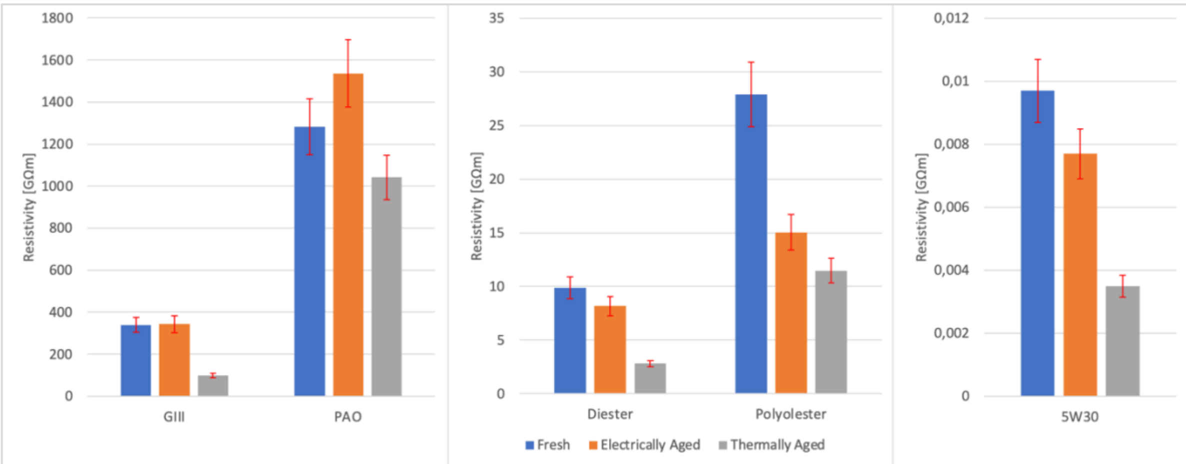

Figure 18: Resistivity of fresh and degraded oil samples.

In general, it can be observed that traditional hydrocarbon-based oils like the GIII mineral oil and the polyalphaolefin have significantly higher resistivity than the ester oils. The ester oils are chemically polar due to the presence of C=O and C–O bonds in their structure and the polarity of these molecules allows the fluid to carry charge more easily, thus resulting in a lower resistivity. Both the PAO and GIII oils are non-polar, but the results show that the PAO's resistivity is more than triple that of the GIII mineral oil. Due to the synthetic nature of PAO, the highly branched hydrocarbon structure is composed of highly regular monomer units and contains no impurities, likely contributing to its higher resistivity.

The effect of electrical degradation on the resistivity of GIII and PAO is relatively insignificant. Although the PAO shows an increase in resistivity following electrical degradation, this change is within the uncertainty range of the readings and therefore the result is inconclusive. It is likely that the apparent increase in resistivity is not as significant as appears, as the dissipation factor of the PAO shows little decrease under electrical degradation. Oxidation of the GIII oil during thermal degradation results in a decreased resistivity due to the increased molecular polarity. A similar trend is shown after thermal degradation of the PAO, but resistivity is decreased to a lesser extent due to a lower degree of oxidation.

For the esters, the spectroscopy results suggest a decrease in the concentration of ester links present in the molecular structure which would result in shorter ester chains. These smaller polar molecules can more easily carry charge when in solution, resulting in a decrease in the resistivity. As shown in the spectroscopy results, thermal degradation resulted in a slightly greater decrease in the peaks corresponding to the ester link signature which would suggest the ester chains are 'broken' or hydrolysed to a greater extent and therefore resistivity is decreased further. The trends of dissipation factor generally correspond with the expected change in resistivity: as dissipation factor increases the resistivity decreases due to the reduction in insulative efficiency of the oil.

Considering the fully formulated 5W30 engine oil as a baseline demonstrates the impact of additive packages on resistivity. Compared with the resistivity of the GIII base oil, the resistivity of the 5W30 engine oil is four orders of magnitude lower. Additive packages involve the blending of various chemicals into the base oil, such as corrosion inhibitors, viscosity stabilisers and anti-oxidants. These additive chemicals alter the properties of the base oil, for example by adding ionic species or polar compounds, which therefore have a dramatic impact on the resistivity. For the formulation of e-thermal fluids, the additive packages will have to be specially designed in order to maintain the required level of resistivity. This consideration goes beyond the scope of this work but is an important area for future research.

4.4.3 Breakdown Voltage

Electrical breakdown of oils is a complex phenomenon that occurs under high voltages, influenced largely by the presence of impurities and moisture in the oil but also by factors such as viscosity and temperature. Various breakdown mechanisms are proposed, the most common being gas dielectric breakdown. The high energy provided to the oil molecules from the applied voltage causes them to collide and form free ions and electrons that are then polarised, forming a conductive chain between the electrodes. As current flows through the conductive chain, the fluid heats up and eventually boils, forming a small gas channel through which an electric breakdown discharge then occurs [45,46]. In e-thermal fluid applications, high breakdown voltage is preferable as a safety precaution to prevent breakdown discharges during battery charging or discharging. The results of the breakdown voltage testing for each of the oil samples are shown in Figure 19, below:

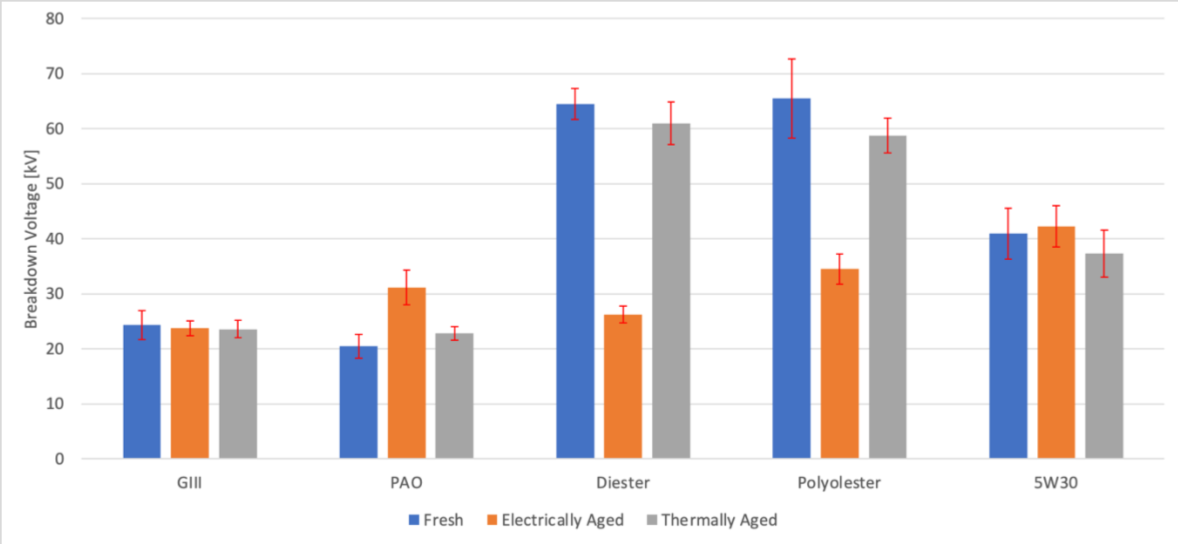

Figure 19: Breakdown voltage of fresh and degraded oil samples.

It can be generally observed that the GIII and PAO oils have lower breakdown voltages when compared with the ester oils. According to the gas dielectric breakdown theory, the BDV will be partly dependent on the energy required to boil the fluid in order to form the small gas channel through which the breakdown spark occurs. This provides an explanation for the higher BDV of the ester oils, as the polar nature of their molecules offers stronger permanent dipole intermolecular forces that result in more energy being required to boil the fluid. Thus, it can be proposed that the breakdown voltage of the esters oils is higher than the PAO and GIII due to their higher boiling points.

While the BDV of GIII and PAO stay relatively constant after degradation, the BDV of the diester and polyolester decrease significantly after electrical degradation. This is likely due to the increase in water content of the esters following electrical degradation, promoting the formation of conductive chains and eventual breakdown discharge at lower applied voltage. The 5W30 engine oil shows moderate breakdown voltage that stays relatively constant after degradation, demonstrating that despite the presence of additives having a dramatic effect on resistivity, their effect on BDV appears to be less significant.

4.5 Decision Matrix for Base Oil Suitability

The decision matrix below ranks the selected base oils based on the results found in this investigation. The ranking is based on the suitability of the stated parameter for e-thermal fluid applications and is assessed both qualitatively and quantitively based on the information available.

Table 2: Decision matrix for the suitability of base oil properties for e-thermal fluid applications.

Decision Parameter	**Ranking** *(1 = least suitable; 4 = most suitable)*			
	GIII	PAO	Diester	Polyolester
Degradation Resistance *Resistance to oxidation and other chemical changes.*	1	3	2	4
Water Content *Low water content that is minimally affected by degradation.*	3	4	1	2
Thermal & Physical Properties *Properties that are minimally affected by degradation and provide a high figure of merit for heat transfer (Mouromtseff number).*	1	2	4	3
Electrical Properties *Low dissipation factor, high resistivity and high BDV that are minimally affected by degradation.*	3	4	1	2
Total Ranking Score	**8**	**13**	**8**	**11**

The decision matrix above is a simple yet effective strategy to weigh-up multiple factors simultaneously when considering the suitability of the base oils for e-thermal fluid applications. The ranking in each category can be logically concluded based on the experimental results and analyses outlined in this report. The outcome of the decision matrix ranking demonstrates that, overall, the polyalphaolefin provides the most suitable thermal, physical and electrical properties for e-thermal fluid applications. However, it should be noted that this decision analysis is limited in its scope in only considering the oil properties and neglected broader factors. Decision parameters such as sustainability, cost and biodegradability have not been considered and further analysis is required to fully characterise these parameters.

5 Conclusions

The aim of this work was to investigate the effects of thermal and electrical degradation on the physical, thermal and electrical properties of the selected base oils to determine their suitability for e-thermal fluid applications. Overall, the following conclusions can be drawn for each of the objectives stated in the introduction:

- From the FTIR spectroscopy results, the PAO showed the least change in chemical structure after thermal and electrical degradation, demonstrating the strongest oxidative resistance. While the PAO showed small amounts of oxidation after thermal degradation, the GIII was oxidised to a greater extent. Degradation of the diester and polyolester resulted in a decrease in the presence of ester links within their chemical structure, suggesting hydrolysis reaction with water.

- The thermal and physical properties of the base oils were minimally changed by degradation, to an extent of less than 11% in all cases. Analysis of the Mouromtseff number revealed that the diester possesses marginally superior heat transfer merit than the other base oils.
- The resistivity of the PAO is far superior to the other base oils, with significantly higher magnitude as well as remaining relatively constant following degradation. Resistivity of the GIII, diester and polyolester were decreased after degradation. The magnitude of resistivity of the ester oils was significantly lower than the hydrocarbon-based oils. An analogous trend was shown by dissipation factor, with PAO showing the lowest while the ester oils showed significantly higher dissipation factors that increased with degradation.
- Overall, it can be concluded that the PAO is the most suitable base oil for e-thermal fluid applications, as demonstrated by the outcome of decision matrix analysis. Its high oxidative resistance, high resistivity, low dissipation factor and effective heat transfer properties make it superior in comparison to the other base oils considered in this work. However, it is important to note that this conclusion is drawn solely based on analysis of the thermal, physical and electrical properties of the base oils. Factors such as cost, biodegradability and sustainability have not been considered in this investigation, and these aspects could greatly influence the base oil suitability.

5.1 Recommendations for Future Work

While this work extensively studied the physical, thermal and electrical properties of base oils, as well as the effects of degradation, it remains limited in its analysis of broader factors that affect the suitability of base oils for e-thermal fluid applications. Factors including material compatibility, base oil sustainability, economic viability and supply chain feasibility have not been considered. Therefore, further work is required to develop a lifecycle analysis of the e-thermal fluids from synthesis to disposal, and such analysis could consider greenhouse gas emissions, oil biodegradability and lifespan of the oil.

Another limitation of this work is its consideration of only the selected base oils and no fully formulated e-thermal fluids with additive packages. Therefore, future work should investigate the impact that additive packages have on the physical, thermal and electrical properties of the fluids as well as their influence over the effects of degradation. The work should aim to optimise the formulation of the additive package for e-thermal fluid applications, to support fluid stability while maintaining effective thermal properties, high resistivity and low dissipation factor.

Whilst analysis of the base oil properties aims to predict the performance in e-thermal fluid applications, practical experimental work is required to analyse a functioning immersion cooled battery system. Future experimental work should set up a 'benchtop model' where the heat transfer efficiency, flow characteristics, electrical characteristics, material compatibility and oil degradation can be analysed in practical application of various e-thermal fluid formulations. This would provide greater insight into how the e-thermal fluids would perform when implemented in EV battery systems and may highlight facets of practical application that the current study was unable to analyse.

6 Reflection & Review

Overall, the project aims were completed successfully, however, some challenges were faced along the way. The main challenge faced in attempting to accurately characterise the electrical properties of the base oils was abnormal water content. Due to the high humidity of Spain's Mediterranean coast, the base oils, especially the ester oils, tended to absorb moisture from the air when samples were left sitting for extended periods. The first set of results obtained for the electrical properties were discarded due to the suspected contamination of the fresh samples with a high content of absorbed water. The property characterisation, along with electrical and thermal degradation, were rerun with fresh samples and particular care was taken to store the samples in containers with minimal air ingress. This delayed the schedule of activities by almost two weeks, but fortunately time had been factored in to allow for this disruption.

The work of this project aligns closely with the ongoing research of PhD students in the CMT research group. The findings and analysis presented in this report will provide some insight and data to support continued research which will incorporate some of the recommendations outlined above. With limited work currently present in literature on the topic of e-thermal fluids, this work and the ongoing research will contribute to the understanding and development of effective and efficient fluids for battery cooling and lubrication of EVs. This work then contributes to the ultimate goal of improving EV technology to make EVs as efficient, as accessible and as safe as possible for consumers. In turn, the increased adoption of EVs over conventional ICE vehicles contributes to the important targets of emissions reductions and attempting to slow the effects global warming.

In terms of the personal learning objectives stated in the introduction, the experience of carrying out my research project on Erasmus exchange has allowed me to fulfil each of these targets. Throughout my 4-months living in Valencia I have had the opportunity to meet new people from all over the world. In times this has pushed me outside of my comfort zone, for example building a new circle of friends and adjusting to different ways of life, but the challenges have brought rewards in growing my confidence and developing my interpersonal skills. Carrying out my research with the CMT department has helped me to develop a concise and clear communication style, by delivering short update presentations to my supervisor on a two-weekly basis. The delays faced during the experimental work have taught me the importance of clear scheduling, prioritising key tasks and contingency planning.

Throughout the project I have continually developed my technical skills in both practical experimental work and data analysis. In the laboratory, I received 'hands-on' training to quickly learn the procedures for operating each piece of analytical equipment within the first few days. After the first couple of weeks, I was almost fully independent in the lab without supervision and was given responsibility for equipment handling, solvent handling, oil sample preparation and equipment cleaning. The results data was handled using Excel and Python, providing a wealth of experience in data organisation, processing and presentation. Python scripts were developed to methodologically process and plot the spectroscopy results, which were exported from the equipment in .csv or .txt files making them more difficult to manage efficiently. Excel was implemented to perform statistical calculations, identify data trends and produce clear plots of results.

Finally, the project has given me the opportunity to implement and develop further my knowledge of chemical engineering principles and practice. Throughout the work I have had to draw on knowledge from previous classes, such as *CP207 Process Analysis and Statistics*, *CP204 Fluid Flow and Heat Transfer*, *CP529 Programming and Optimisation* and *CP540 Project Planning, Management and Methods*. Through extensive background research I was able to gain a thorough understanding of the context and requirements for EV-fluids which helped to give my work clear purpose and motivations. Overall, the project has provided a wealth of experience, developing my academic knowledge, my personal skills and my technical abilities. My personal growth and development throughout this experience will be carried forward into the workplace, where I hope to make a positive impact and effectively contribute to future engineering projects.

6.1 Budget

The budget to follow summarises the costs associated with this work. The costs are broken into three categories: human resource costs, equipment costs and material costs. Human resource costs are estimated based on the hourly salary of the staff member and the number of active hours they invested into the project or associated activities. The equipment costs are estimated based on the total cost of the equipment scaled for the actual hours of use. Base oil costs are quoted for the volume purchased, and it should be noted that the ester oils were provided free of charge to the laboratory as samples to be tested.

6.1.1 Human Resource Costs

Table 3, below, shows the costs associated with salaried staff that have contributed their time towards this project:

Table 3: Human resource costs associated with this work.

Job Title	Hourly Salary (€/hour)	Hours Contributed	Cost (€)
Full Professor	74	30	2220
Senior Technician	33	10	330
		Total Cost	**2550**

6.1.2 Equipment Costs

Table 4, below, shows the costs associated with the laboratory equipment used throughout this project. Note that the actual cost of the equipment has been estimated based on the total equipment cost, the actual hours of use and the estimated expected lifetime of the equipment as shown in Equation 4:

$$Actual\ Equip.Cost = \frac{Usage\ Time}{Equip.\ Lifetime} \times Total\ Equip.Cost \tag{4}$$

Table 4: Equipment costs associated with this work.

Item	Total Equipment Cost (€)	Equipment Lifetime (hrs)	Equipment Use Time (hrs)	Actual Equipment Cost (€)
Huazheng HZJQ-X1 Transformer Oil BDV Tester	€3000	5000	300	180
DF9010 Oil Dissipation Factor & Resistivity Test System	€13000	5000	300	780
Thermtest THW-L1 System	€50000	5000	150	1500
Anton Parr Density & Viscosity Equipment	€30000	5000	100	600
A2 Technologies FTIR Equipment	€15000	5000	50	150
Karl Fischer Water Content Coulometric Titration Equipment	€2500	5000	100	50

Thermal Bath	€1000	5000	250	50
			Total Cost	**3310**

6.1.3 Material Costs

Table 5, below, shows the costs associated with the materials used throughout the project, including base oil samples and other laboratory items.

Table 5: Material costs associated with this work.

Item		**Cost (€)**
Lab Supplies (glassware, solvents, etc.)		500
Silicon Oil, 15 L (thermal bath)		250
Yubase 4 Oil, 20 L (GIII base oil)		60
Espectrasyn 4 Oil, 20 L (PAO base oil)		100
	Total Cost	**910**

6.1.4 Total Costs

Table 6, below, summarises the overall total cost associated with human resources, equipment and materials used throughout this project.

Table 6: Overall total cost associated with this work.

Cost Category		**Cost (€)**
Human resources		2550
Equipment		3310
Materials		910
	Overall total cost	**6770**

7 References

[1] Universitat Politècnica de València (UPV). "The UPV in the rankings." http://www.upv.es/rankings/index-en.html (accessed 25/03/2023).

[2] International Energy Agency (IEA), "Global EV Outlook 2022," IEA, Paris, 2022. [Online]. Available: https://www.iea.org/reports/global-ev-outlook-2022

[3] European Environment Agency (EEA). "New registrations of electric vehicles in Europe." https://www.eea.europa.eu/ims/new-registrations-of-electric-vehicles (accessed 13/02/2023).

[4] International Energy Agency (IEA), "Transport," IEA, Paris, 2022. [Online]. Available: https://www.iea.org/reports/transport

[5] International Energy Agency (IEA), "Global Energy Review: CO2 Emissions in 2021," IEA, Paris, 2022. [Online]. Available: https://www.iea.org/reports/global-energy-review-co2-emissions-in-2021-2

[6] European Parliament, "EU ban on the sale of new petrol and diesel cars from 2035 explained." [Online]. Available: https://www.europarl.europa.eu/news/en/headlines/economy/20221019STO44572/eu-ban-on-sale-of-new-petrol-and-diesel-cars-from-2035-explained

[7] R. I. Taylor, "Energy Efficiency, Emissions, Tribological Challenges and Fluid Requirements of Electrified Passenger Car Vehicles," *Lubricants,* vol. 9, no. 7, p. 66, 2021. [Online]. Available: https://www.mdpi.com/2075-4442/9/7/66.

[8] D. W. Sundin and S. Sponholtz, "Thermal Management of Li-Ion Batteries With Single-Phase Liquid Immersion Cooling," *IEEE Open Journal of Vehicular Technology,* vol. 1, pp. 82-92, 2020, doi: 10.1109/OJVT.2020.2972541.

[9] TotalEnergies. "What is motor oil used for and what are its benefits?" https://services.totalenergies.uk/what-is-motor-oil-used-for-benefits (accessed 22/02/23).

[10] Lubes'n'Greases, "Perspective on Electric Vehicles," LNG Publishing Company, 2019. [Online]. Available: www.LubesnGreases.com

[11] J. Mitar *et al.*, "Lubricating oils for modern automatic transmissions of motor vehicles," presented at the COMETA 2016 Conference on Mechanical Engineering Technologies and Applications, Bosnia and Herzegovina, 2016. [Online]. Available: https://www.researchgate.net/publication/311677822_Lubricating_oils_for_modern_automatic_transmissions_of_motor_vehicles.

[12] S. S. Rawat and A. P. Harsha, "Current and Future Trends in Grease Lubrication," in *Automotive Tribology*, J. K. Katiyar, S. Bhattacharya, V. K. Patel, and V. Kumar Eds. Singapore: Springer Singapore, 2019, pp. 147-182.

[13] Transparency Market Research, "EV Lightweight Materials Market," 2022. [Online]. Available: https://www.transparencymarketresearch.com/ev-lightweight-materials-market.html

[14] Shell, "Electric Vehicle Fluids," in "Shell White Paper Reports," 2019. [Online]. Available: https://www.shell.com/content/dam/shell/assets/en/business-functions/shell-lubricants/documents/shell-white-paper.pdf

[15] S. Lv *et al.*, "The Influence of Temperature on the Capacity of Lithium Ion Batteries with Different Anodes," *Energies,* vol. 15, no. 1, p. 60, 2022. [Online]. Available: https://www.mdpi.com/1996-1073/15/1/60.

[16] J.-W. Han *et al.*, "Experimental Study on Dielectric Fluid Immersion Cooling for Thermal Management of Lithium-Ion Battery," *Symmetry,* vol. 14, no. 10, p. 2126, 2022. [Online]. Available: https://www.mdpi.com/2073-8994/14/10/2126.

[17] S. Ma *et al.*, "Temperature effect and thermal impact in lithium-ion batteries: A review," *Progress in Natural Science: Materials International,* vol. 28, no. 6, pp. 653-666, 2018/12/01/ 2018, doi: https://doi.org/10.1016/j.pnsc.2018.11.002.

[18] Dober. "Cooling Electric Vehicles." https://www.dober.com/electric-vehicle-cooling-systems (accessed 23/02/23).

[19] H. Liu *et al.*, "Thermal issues about Li-ion batteries and recent progress in battery thermal management systems: A review," *Energy Conversion and Management,* vol. 150, pp. 304-330, 2017/10/15/ 2017, doi: https://doi.org/10.1016/j.enconman.2017.08.016.

[20] D. Chen *et al.*, "Comparison of different cooling methods for lithium ion battery cells," *Applied Thermal Engineering,* vol. 94, pp. 846-854, 2016/02/05/ 2016, doi: https://doi.org/10.1016/j.applthermaleng.2015.10.015.

[21] W. Wu *et al.*, "A critical review of battery thermal performance and liquid based battery thermal management," *Energy Conversion and Management,* vol. 182, pp. 262-281, 2019/02/15/ 2019, doi: https://doi.org/10.1016/j.enconman.2018.12.051.

[22] P. Dubey, G. Pulugundla, and A. K. Srouji, "Direct Comparison of Immersion and Cold-Plate Based Cooling for Automotive Li-Ion Battery Modules," *Energies,* vol. 14, no. 5, p. 1259, 2021. [Online]. Available: https://www.mdpi.com/1996-1073/14/5/1259.

[23] S. Yang *et al.*, "Essential technologies on the direct cooling thermal management system for electric vehicles," *International Journal of Energy Research,* vol. 45, no. 10, pp. 14436-14464, 2021, doi: https://doi.org/10.1002/er.6775.

[24] Q. L. Yue *et al.*, "Advances in thermal management systems for next-generation power batteries," *International Journal of Heat and Mass Transfer,* vol. 181, p. 121853, 2021/12/01/ 2021, doi: https://doi.org/10.1016/j.ijheatmasstransfer.2021.121853.

[25] X. Feng *et al.*, "Thermal runaway mechanism of lithium ion battery for electric vehicles: A review," *Energy Storage Materials,* vol. 10, pp. 246-267, 2018/01/01/ 2018, doi: https://doi.org/10.1016/j.ensm.2017.05.013.

[26] Q. Wang *et al.*, "Thermal runaway caused fire and explosion of lithium ion battery," *Journal of Power Sources,* vol. 208, pp. 210-224, 2012/06/15/ 2012, doi: https://doi.org/10.1016/j.jpowsour.2012.02.038.

[27] Croda Internation Plc. "Battery cooling and thermal management." https://www.crodaenergytechnologies.com/en-gb/applications/battery-technologies/battery-cooling-and-thermal-management (accessed 24/02/2023).

[28] L. S. Oumert *et al.*, "Comparative study of the degradation rate of new and regenerated mineral oils following electrical stress," *IET Generation, Transmission & Distribution,* vol. 12, no. 21, pp. 5891-5897, 2018, doi: https://doi.org/10.1049/iet-gtd.2018.6077.

[29] N. A. Pambudi *et al.*, "The immersion cooling technology: Current and future development in energy saving," *Alexandria Engineering Journal,* vol. 61, no. 12, pp. 9509-9527, 2022/12/01/ 2022, doi: https://doi.org/10.1016/j.aej.2022.02.059.

[30] D. N. Canter. "Heat transfer fluids: Growing in visibility and importance." Society of Tribologists and Lubrication Engineers (STLE). https://www.stle.org/files/TLTArchives/2021/12_December/Cover_Story.aspx?utm_source=Real (accessed 06/02/2023).

[31] E. Agamloh, A. von Jouanne, and A. Yokochi, "An Overview of Electric Machine Trends in Modern Electric Vehicles," *Machines,* vol. 8, no. 2, p. 20, 2020. [Online]. Available: https://www.mdpi.com/2075-1702/8/2/20.

[32] *API 1509, Appendix E, Section E1.3*, American Petroleum Institute, 2011. [Online]. Available: https://www.stle.org/images/pdf/STLE_ORG/BOK/OM_OA/Base%20Oils/Base%20Oil%20Groups_Manufacture_Prop_Perform_April15%20TLT.pdf

[33] S. F. Brown. (2015) Base Oil Groups: Manufacture, Properties and Performance. *TRIBOLOGY & LUBRICATION TECHNOLOGY*. Available: https://www.stle.org/images/pdf/STLE_ORG/BOK/OM_OA/Base%20Oils/Base%20Oil%20Groups_Manufacture_Prop_Perform_April15%20TLT.pdf

[34] S. A. Khan, A. A. Khan, and M. Tariq, "Measurement of Tan-delta and DC Resistivity of Synthetic Ester Based Oil Filled with Fe2O3, TiO2 and Al2O3 Nanoparticles," *Smart Science,* vol. 9, no. 3, pp. 216-225, 2021/07/03 2021, doi: 10.1080/23080477.2021.1920130.

[35] A. Garg *et al.*, "Compatibility of ester oil with transformer components and comparison with mineral oil," in *2019 IEEE 4th International Conference on Condition Assessment Techniques in Electrical Systems (CATCON)*, 21-23 Nov. 2019 2019, pp. 1-6, doi: 10.1109/CATCON47128.2019.CN0011.

[36] Engineered Fluids. "AmpCool™ Engineered for Liquid Immersion Cooling of Batteries, Electric Motors & EMCs." https://www.engineeredfluids.com/products/ampcool/?utm_term=liquid%20cooling%20for%20batteries&utm_campaign=Engineered+Fluids&utm_source=adwords&utm_medium=ppc (accessed 13/03/2023).

[37] 3M. "One and two phase immersion cooling of high power components." https://www.3m.co.uk/3M/en_GB/novec-uk/applications/thermal-management/immersion-cooling-of-power-electronics/ (accessed 12/03/2023).

[38] Solvay. "Galden® PFPE." https://www.solvay.com/en/brands/galden-pfpe (accessed 13/03/2023).

[39] M&I Materials Ltd. "MIVOLT EV Battery Systems." https://mivoltcooling.com/applications/ev-battery-systems/ (accessed 13/03/2023).

[40] ExxonMobil, "How Synthetic Base Oils can help create novel e-Mobility fluid formulations," in "White Paper," 2018. [Online]. Available: https://go.exxonmobilchemical.com/l/562282/2020-02-26/ddf3cm?_ga=2.163162490.750221651.1632310962-527938678.1626109431

[41] K. V. Jithin and P. K. Rajesh, "Numerical analysis of single-phase liquid immersion cooling for lithium-ion battery thermal management using different dielectric fluids," *International Journal of Heat and Mass Transfer,* vol. 188, p. 122608, 2022/06/01/ 2022, doi: https://doi.org/10.1016/j.ijheatmasstransfer.2022.122608.

[42] S. Hurley *et al.*, "Understanding Base Oils and Lubricants for Electric Drivetrain Applications," 2019. [Online]. Available: https://doi.org/10.4271/2019-01-2337.

[43] N. Rivera *et al.*, "Cooling Performance of Fresh and Aged Automatic Transmission Fluids for Hybrid Electric Vehicles," *Applied Sciences,* vol. 12, no. 17, p. 8911, 2022. [Online]. Available: https://www.mdpi.com/2076-3417/12/17/8911.

[44] B. C. Smith, "The C=O Bond, Part VII: Aromatic Esters, Organic Carbonates, and More of the Rule of Three," *Spectroscopy*, vol. 33, no. 9. [Online]. Available: https://www.spectroscopyonline.com/view/co-bond-part-vii-aromatic-esters-organic-carbonates-and-more-rule-three

[45] Kingrun Transformer Instrument Co. "What is the breakdown voltage of transformer oil?" https://www.kritester.com/new/what-is-the-breakdown-voltage-of-transformer-oil.html (accessed 24/03/2023).

[46] GlobeCore. "Transformer Oil Breakdown Voltage Measurements." https://globecore.com/instruments/transformer-oil-breakdown-voltage-measurements/ (accessed 24/03/2023).

Appendix A – Sample Calculation of Uncertainties

The sample calculation below is shown for the calculation of the total reported uncertainty within the averaged measurement of breakdown voltage for the fresh Group III oil. The equipment measuring uncertainty associated with the Huazheng HZJQ-X1 Transformer Oil BDV Tester is ($\pm$reading $\times$ 3%), as stated in Table 1.

Firstly, the mean (μ) of the repeated measurements was calculated:

$$\mu = \frac{\sum x_i}{N} = \frac{(17.46 + 27.13 + 30.39 + 19.40 + 27.14)}{5} = 24.304 \text{ kV}$$

Where $\sum x_i$ is the sum of the measured values and N is the number of measurements recorded. The equipment measurement uncertainty (σ_{equip}) associated with this mean value is calculated based on the manufacturers specification:

$$\sigma_{equip} = \pm reading \times 0.03 = \pm 24.30 \times 0.03 = \pm 0.729 \text{ kV}$$

The standard deviation (S) of the repeated BDV measurements was then calculated using the general formula below:

$$S = \sqrt{\frac{\sum (x_i - \mu)^2}{N}}$$

Substituting numbers into this equation yields the following results:

$$S = \sqrt{\frac{(17.46 - 24.304)^2 + (27.13 - 24.304)^2 + (30.39 - 24.304)^2 + (19.4 - 24.304)^2 + (17.46 - 24.304)^2}{5}}$$

$$S = 5.567 \text{ kV}$$

The standard error (σ_{SE}) is then calculated as follows:

$$\sigma_{SE} = \pm \frac{S}{\sqrt{N}} = \pm \frac{5.567}{\sqrt{5}} = \pm 2.490$$

The total error is then calculated by combining the equipment measurement error and the standard error according to the general principles of error propagation:

$$\sigma_{total} = \pm \sqrt{\sigma_{equip}^2 + \sigma_{SE}^2} = \pm \sqrt{(0.729 \ldots)^2 + (2.489 \ldots)^2} = \pm 2.594 \text{ kV}$$

Appendix B – Raw Experimental Data

A.1 – Thermal and Physical Properties

Table B-1: Raw data for thermal and physical properties of the fresh oil samples.

	°C	mm²/s	mPa·s	g/cm³	W/mK	MJ/m³K	kJ/kg K	
		FRESH						
	Temperature	KV	DV	D	TC	VSHC	SHC	Mo
Group III	20	44,763	37,086	0,8285	0,1381	1,8307	2,20971277	13,6384245
	30	28,797	23,675	0,8221	0,1367	1,8475	2,24726744	16,7108644
	40	19,594	15,985	0,8158	0,1355	1,8607	2,28086707	19,9579444
	50	13,993	11,327	0,8094	0,1336	1,8671	2,30675689	23,1869072
	60	10,428	8,3761	0,8032	0,1322	1,8897	2,35276449	26,5393286
	70	8,006	6,3809	0,7969	0,1304	1,8966	2,37998042	29,8121466
	80	6,3498	5,0205	0,7907	0,1290	1,9085	2,41367468	33,0788311
	90	5,1628	4,0493	0,7843	0,1281	1,9510	2,48750824	36,5369223
	100	4,2899	3,3375	0,778	0,1268	1,9643	2,52478586	39,6766186
	110	3,6329	2,8032	0,7716	0,1261	1,9888	2,57748927	42,9306372
	120	3,1294	2,3948	0,7653	0,1244	2,0086	2,6246162	45,7850549

	°C	mm²/s	mPa·s	g/cm³	W/mK	MJ/m³K	MJ/kg K	
		FRESH						
	Temperature	KV	DV	D	TC	VSHC	SHC	Mo
PAO	20	39,567	32,291	0,81612	0,1445	1,8889	2,31446542	15,0497234
	30	25,977	21,035	0,80977	0,1427	1,9015	2,34819875	18,2234818
	40	17,896	14,378	0,80346	0,1411	1,9151	2,38358635	21,6030734
	50	12,922	10,299	0,79703	0,1397	1,9289	2,42016659	25,065817

	60	9,6741	7,6501	0,79078	0,1378	1,9432	2,4573119	28,5214308
	70	7,4975	5,8817	0,78449	0,1358	1,9563	2,49372415	31,9221471
	80	5,9497	4,6280	0,77785	0,1347	1,9696	2,53212486	35,456851
	90	4,8417	3,7373	0,77189	0,1329	1,9923	2,58103445	38,8624421
	100	4,0297	3,0826	0,76498	0,1312	2,0066	2,62306765	42,1081905
	110	3,4143	2,5905	0,75872	0,1294	2,0184	2,66030567	45,1932169
	120	2,9397	2,2126	0,75266	0,1282	2,0415	2,71241707	48,3620994

	°C	mm²/s	mPa·s	g/cm³	W/mK	MJ/m³K	MJ/kg K	
		FRESH						
	Temperature	KV	DV	D	TC	VSHC	SHC	Mo
Diester	20	23,29	21,284	0,9138	0,1456	1,8972	2,07619212	19,430873
	30	16,066	14,569	0,9068	0,1441	1,9151	2,11190477	23,0532476
	40	11,639	10,468	0,8993	0,1424	1,9260	2,14166868	26,6517892
	50	8,7878	7,8403	0,8922	0,1409	1,9429	2,17763455	30,2941994
	60	6,8687	6,0782	0,8849	0,1393	1,9533	2,20741679	33,8184526
	70	5,5113	4,8382	0,8779	0,1376	1,9698	2,24375196	37,2865324
	80	4,5289	3,9434	0,8707	0,1359	1,9842	2,27882364	40,6498175
	90	3,8001	3,2815	0,8635	0,1344	2,0022	2,31869106	43,9460316
	100	3,2444	2,7784	0,8563	0,1326	2,0167	2,35508638	47,0364821
	110	2,8123	2,3881	0,8492	0,1309	2,0308	2,39139763	49,991325
	120	2,4704	2,0799	0,8419	0,1292	2,0449	2,42889113	52,7851228

	°C	mm²/s	mPa·s	g/cm³	W/mK	MJ/m³K	MJ/kg K	
		FRESH						
	Temperature	KV	DV	D	TC	VSHC	SHC	Mo

Polyolester	20	44,237	41,677	0,94213	0,1490	1,9331	2,05186194	14,6877402
	30	28,842	26,961	0,93480	0,1475	1,9460	2,08174955	17,8788899
	40	19,841	18,389	0,92683	0,1456	1,9597	2,11445102	21,1779751
	50	14,296	13,140	0,91917	0,1438	1,9727	2,14614676	24,5559438
	60	10,674	9,7489	0,91333	0,1425	1,9878	2,1764385	28,0671613
	70	8,2534	7,4787	0,90614	0,1408	2,0011	2,20833659	31,4818278
	80	6,5652	5,9029	0,89912	0,1389	2,0160	2,24220913	34,8270873
	90	5,3526	4,7736	0,89182	0,1371	2,0296	2,27584599	38,0909865
	100	4,4543	3,9407	0,88469	0,1357	2,0483	2,31528294	41,3697308
	110	3,7746	3,3122	0,87751	0,1339	2,0648	2,35307109	44,4406221
	120	3,2532	2,8319	0,87051	0,1324	2,0847	2,3948338	47,4513727

	°C	mm²/s	mPa·s	g/cm³	W/mK	MJ/m³K	MJ/kg K	
		FRESH						
	Temperature	KV	DV	D	TC	VSHC	SHC	Mo
5W30	20	168,03	143,13	0,85179	0,1404	1,8583	2,18161092	7,44137941
	30	101,76	86,170	0,84677	0,1389	1,8739	2,21293862	9,37825871
	40	65,778	55,308	0,84082	0,1374	1,8842	2,24094443	11,4461842
	50	44,709	37,316	0,83464	0,1362	1,9048	2,28223973	13,6951422
	60	31,907	26,432	0,82840	0,1348	1,9191	2,31668766	15,9746698
	70	23,606	19,338	0,81922	0,1333	1,9344	2,36128512	18,316947
	80	18,061	14,720	0,81501	0,1320	1,9568	2,40100802	20,7184609
	90	14,553	11,522	0,80973	0,1306	1,9724	2,43593529	23,0701576
	100	11,498	9,2254	0,80235	0,1292	1,9875	2,47706558	25,3743943
	110	9,4774	7,5482	0,79645	0,1278	2,0088	2,52224648	27,6942398
	120	7,9714	6,3008	0,79042	0,1267	2,0310	2,56946222	29,9657425

Table B-2: Raw data for thermal and physical properties of the thermally aged oil samples.

	°C	mm²/s	mPa·s	g/cm³	W/mK	MJ/m³K	kJ/kg K	
		T_AGED						
	Temperature	KV	DV	D	TC	VSHC	SHC	Mo
Group III	20	45,219	37,512	0,8296	0,1387	1,8422	2,2206421	13,636666
	30	28,82	23,727	0,8233	0,1373	1,8519	2,24935115	16,7711982
	40	19,746	16,129	0,8168	0,1358	1,8704	2,28992981	19,9497267
	50	14,094	11,424	0,8105	0,1343	1,8853	2,32611565	23,2562904
	60	10,468	8,4187	0,8042	0,1327	1,8981	2,36020961	26,5973216
	70	8,0533	6,4256	0,7979	0,1312	1,9125	2,39690406	29,9261604
	80	6,3913	5,0591	0,7916	0,1299	1,9318	2,44034258	33,2471993
	90	5,1949	4,079	0,7852	0,1281	1,9474	2,4801733	36,4216306
	100	4,3148	3,3608	0,7789	0,1269	1,9628	2,52000561	39,5878599
	110	3,6536	2,8224	0,7725	0,1254	1,9832	2,56726521	42,6131555
	120	3,1454	2,4102	0,7662	0,1244	2,0057	2,61769469	45,6373586

	°C	mm²/s	mPa·s	g/cm³	W/mK	MJ/m³K	MJ/kg K	
		T_AGED						
	Temperature	KV	DV	D	TC	VSHC	SHC	Mo
PAO	20	45,235	37,515	0,82934	0,1406	1,8519	2,23300751	13,7826144
	30	29,039	23,899	0,82298	0,1391	1,8692	2,27122839	16,9095071
	40	19,77	16,145	0,81667	0,1374	1,8842	2,30715153	20,1447054
	50	14,093	11,419	0,81021	0,1361	1,9023	2,34790042	23,5362887
	60	10,488	8,4263	0,80344	0,1346	1,9181	2,38731819	26,9138539
	70	8,0612	6,431	0,79777	0,1329	1,9317	2,42138342	30,2806407
	80	6,3879	5,0558	0,79147	0,1317	1,9481	2,46140197	33,6570382

	90	5,1919	4,0765	0,78517	0,1302	1,9626	2,4996138	36,9104025
	100	4,312	3,3585	0,77887	0,1286	1,9822	2,54498238	40,0751966
	110	3,6516	2,8208	0,77248	0,1268	1,9985	2,58718441	43,0424072
	120	3,1436	2,4088	0,7663	0,1256	2,0152	2,62975018	46,0254917

	°C	*mm²/s*	*mPa·s*	*g/cm³*	*W/mK*	*MJ/m³K*	*MJ/kg K*	
		T_AGED						
	Temperature	KV	DV	D	TC	VSHC	SHC	Mo
Diester	20	24,147	22,107	0,91553	0,1463	1,9110	2,08732884	19,2138439
	30	16,568	15,051	0,90839	0,1449	1,9263	2,12053556	22,8450248
	40	11,962	10,780	0,90119	0,1433	1,9374	2,14977495	26,4824296
	50	8,9943	8,0409	0,89400	0,1415	1,9495	2,18061214	30,0863391
	60	6,9867	6,1954	0,88673	0,1400	1,9666	2,21775746	33,7365813
	70	5,6171	4,9402	0,87949	0,1382	1,9803	2,25167726	37,139352
	80	4,6142	4,0257	0,87246	0,1366	1,9873	2,27779724	40,4645021
	90	3,8673	3,3460	0,86521	0,1350	2,0131	2,32670402	43,7964776
	100	3,2985	2,8304	0,85809	0,1333	2,0276	2,36297371	46,9073427
	110	2,8570	2,4311	0,85095	0,1316	2,0451	2,40328703	49,9004256
	120	2,5075	2,1162	0,84393	0,1305	2,0533	2,43305821	52,8315223

	°C	*mm²/s*	*mPa·s*	*g/cm³*	*W/mK*	*MJ/m³K*	*MJ/kg K*	
		T_AGED						
	Temperature	KV	DV	D	TC	VSHC	SHC	Mo
Polyolester	20	45,650	43,080	0,94370	0,1501	1,9440	2,06002516	14,5691105
	30	29,623	27,741	0,93647	0,1485	1,9602	2,09322483	17,7749316
	40	20,328	18,875	0,92855	0,1467	1,9712	2,12285285	21,0834976

	50	14,583	13,447	0,92208	0,1447	1,9763	2,14325845	24,4427218
	60	10,890	9,9636	0,91492	0,1433	1,9842	2,16867466	27,8915834
	70	8,4101	7,6278	0,90699	0,1415	2,0098	2,21590419	31,3597359
	80	6,6716	6,0085	0,90061	0,1398	2,0252	2,24864699	34,7722812
	90	5,4324	4,8544	0,89361	0,1384	2,0477	2,29150444	38,1864503
	100	4,5301	4,0160	0,88652	0,1367	2,0557	2,31879136	41,2963453
	110	3,8278	3,3657	0,87928	0,1348	2,0687	2,35273178	44,3631809
	120	3,2954	2,8736	0,87201	0,1332	2,0795	2,38472036	47,3026316

	°C	*mm²/s*	*mPa·s*	*g/cm³*	*W/mK*	*MJ/m³K*	*MJ/kg K*	
		T_AGED						
	Temperature	KV	DV	D	TC	VSHC	SHC	Mo
5W30	20	183,26	156,63	0,85469	0,1414	1,8613	2,17775739	7,18249535
	30	110,2	93,491	0,84834	0,1399	1,8792	2,21518481	9,08414869
	40	70,661	59,498	0,84202	0,1385	1,8932	2,24841392	11,1467005
	50	47,72	39,877	0,83565	0,1372	1,9103	2,28595001	13,359778
	60	33,654	27,910	0,82931	0,1358	1,9259	2,32230858	15,6736432
	70	25,024	20,596	0,82304	0,1342	1,9407	2,3579776	17,9206986
	80	19,051	15,548	0,81614	0,1331	1,9580	2,39909246	20,3183525
	90	14,937	12,092	0,80954	0,1317	1,9752	2,43986506	22,6816145
	100	12,045	9,6549	0,80157	0,1302	1,9979	2,49243014	25,0032479
	110	10,194	8,1038	0,79496	0,1288	2,0130	2,53222593	26,9194447
	120	8,3862	6,6112	0,78834	0,1278	2,0368	2,58363788	29,4639176

Table B-3: Raw data for thermal and physical properties of the electrically aged oil samples.

	°C	mm²/s	mPa·s	g/cm³	W/mK	MJ/m³K	kJ/kg K	
		E_AGED						
	Temperature	KV	DV	D	TC	VSHC	SHC	Mo
Group III	20	44,5780	36,9550	0,8290	0,138	1,83043	2,20800	13,6544981
	30	28,8430	23,7230	0,8225	0,13635	1,84810	2,24693	16,6733363
	40	19,4700	15,8920	0,8162	0,13512	1,86619	2,28644	19,9980691
	50	14,0230	11,3580	0,8099	0,13375	1,88042	2,32179	23,2322796
	60	10,4270	8,3800	0,8037	0,13254	1,89367	2,35619	26,6043322
	70	8,0133	6,3897	0,7974	0,13107	1,91210	2,39792	29,9804204
	80	6,3468	5,0206	0,7911	0,12989	1,92925	2,43869	33,3493633
	90	5,1550	4,0454	0,7848	0,12878	1,94831	2,48256	36,6817831
	100	4,2833	3,3341	0,7784	0,12724	1,97120	2,53237	39,8496358
	110	3,6254	2,7984	0,7721	0,12631	1,99321	2,58154	43,0501589
	120	3,1225	2,3911	0,7658	0,12482	2,01112	2,62617	45,9449959

	°C	mm²/s	mPa·s	g/cm³	W/mK	MJ/m³K	MJ/kg K	
		E_AGED						
	Temperature	KV	DV	D	TC	VSHC	SHC	Mo
PAO	20	39,2080	32,0190	0,8166	0,1424	1,87027	2,29031	14,9170475
	30	25,9450	21,0170	0,8101	0,14051	1,88311	2,32454	17,9919295
	40	17,7890	14,3000	0,8039	0,13885	1,89604	2,35855	21,3615337
	50	12,9030	10,2900	0,7975	0,13746	1,91500	2,40125	24,7555194
	60	9,6672	7,6495	0,7913	0,13622	1,92148	2,42826	28,2133098
	70	7,4724	5,8657	0,7850	0,13464	1,93688	2,46736	31,678817
	80	5,9322	4,6189	0,7786	0,13334	1,95954	2,51675	35,214296

	90	4,8274	3,7280	0,7723	0,13185	1,97558	2,55805	38,6099
	100	4,0131	3,0732	0,7658	0,13077	1,98718	2,59491	41,9609444
	110	3,3996	2,5815	0,7594	0,12883	2,01194	2,64938	45,0967901
	120	2,9307	2,2069	0,7530	0,12772	2,03290	2,69973	48,2378059

	°C	mm²/s	mPa·s	g/cm³	W/mK	MJ/m³K	MJ/kg K	
		E_AGED						
	Temperature	KV	DV	D	TC	VSHC	SHC	Mo
Diester	20	23,081	21,107	0,9145	0,14453	1,88705	2,06348	19,3845744
	30	16,023	14,533	0,907	0,14271	1,90557	2,10096	22,8908077
	40	11,518	10,364	0,8998	0,14126	1,92100	2,13492	26,6212001
	50	8,7528	7,8121	0,8925	0,13987	1,93971	2,17334	30,1837791
	60	6,8377	6,0543	0,8854	0,13837	1,94928	2,20158	33,7087089
	70	5,4746	4,808	0,8782	0,13677	1,96399	2,23638	37,2233491
	80	4,5049	3,924	0,871	0,13515	1,98124	2,27467	40,5874621
	90	3,7806	3,2657	0,8638	0,13417	1,99866	2,31380	43,9863904
	100	3,2282	2,7656	0,8567	0,13235	2,01541	2,35253	47,0742584
	110	2,7992	2,378	0,8495	0,13096	2,03395	2,39429	50,1328526
	120	2,458	2,0704	0,8423	0,12979	2,05851	2,44392	53,1824088

	°C	mm²/s	mPa·s	g/cm³	W/mK	MJ/m³K	MJ/kg K	
		E_AGED						
	Temperature	KV	DV	D	TC	VSHC	SHC	Mo
Polyolester	20	43,627	41,12	0,9425	0,14764	1,92428	2,04168	14,671768
	30	28,588	26,709	0,9353	0,14587667	1,93498	2,06884	17,7947474
	40	19,54	18,133	0,928	0,14436667	1,94956	2,10082	21,1733113

	50	14,16	13,039	0,9208	0,14274	1,96174	2,13047	24,4968382
	60	10,605	9,6883	0,9136	0,14157	1,97596	2,16283	27,9754278
	70	8,2069	7,4402	0,9066	0,13984667	1,99239	2,19766	31,3849491
	80	6,5311	5,8742	0,8994	0,13810333	2,00913	2,23386	34,7441494
	90	5,3233	4,7497	0,8923	0,13708333	2,02637	2,27095	38,1684105
	100	4,4273	3,9179	0,885	0,13566667	2,04731	2,31335	41,4740271
	110	3,7518	3,2933	0,8778	0,13399667	2,06527	2,35278	44,5866108
	120	3,2316	2,8135	0,8706	0,13256333	2,08437	2,39417	47,6270777

	°C	mm²/s	mPa·s	g/cm³	W/mK	MJ/m³K	MJ/kg K	
		E_AGED						
	Temperature	KV	DV	D	TC	VSHC	SHC	Mo
5W30	20	207,59	177,09	0,8531	0,13712667	1,82976	2,14483	6,59751157
	30	122,86	104,04	0,8468	0,13567	1,84233	2,17564	8,40056435
	40	77,259	64,938	0,8405	0,13469666	1,86187	2,21519	10,4330346
	50	51,548	43,005	0,8343	0,1335	1,87988	2,25324	12,583534
	60	36,007	29,814	0,828	0,13246333	1,89709	2,29117	14,8617463
	70	26,277	21,593	0,8218	0,13114667	1,91700	2,33269	17,1781319
	80	19,851	16,189	0,8155	0,13019333	1,93921	2,37794	19,576119
	90	15,455	12,507	0,8092	0,1291	1,95600	2,41721	21,9582015
	100	12,356	9,9213	0,803	0,12776334	1,97712	2,46216	24,3115033
	110	10,105	8,0501	0,7967	0,12667333	2,00036	2,51081	26,6714559
	120	8,4306	6,6626	0,7903	0,12561333	2,01576	2,55062	28,951318

A.2 – Electrical Properties

Table B-4: Raw data for electrical properties of the fresh oil samples.

	FRESH						
Group III	**PROPERTIES**	**BDV**	**Rho**	**Tan delta 50Hz**	**Tan delta 60Hz**	**C**	**e**
	UNITS	**KV**	**G Ohm*m**	**%**	**%**	**pF**	
	1	17,46	307,00	0,7874	0,6562	121,2	2,03
	2	27,13	326,00	0,5377	0,448	121,3	2,036
	3	30,39	363,00	0,4614	0,3845	121,3	2,035
	4	19,4	376,00	0,4297	0,358	121,3	2,04
	5	27,14	295,00	0,7666	0,6388	121,3	2,04
	6	–	333	0,4699	0,3916	121,3	2,036
	7	–	351	0,4335	0,3613	121,3	2,036
	8	–	362	0,431	0,3592	121,2	2,034
	AVERAGE	24,304	339,125	0,53965	0,4497	121,275	2,03575
	STD_DEV	5,56682405	28,7423903	0,15073152	0,12560954	0,046291	0,00190863
	STD ERROR	2,4895594	10,1619695	0,05329164	–	–	–
	EQUIP ERROR	0,72912	33,9125	0,0063965	–	–	–
	TOTAL ERROR	2,59413222	35,4023062	0,05367415	–	–	–
PAO	**PROPERTIES**	**BDV**	**Rho**	**Tan delta 50Hz**	**Tan delta 60Hz**	**C**	**e**
	UNITS	**KV**	**G Ohm*m**	**%**	**%**	**pF**	
	1	14,38	1350	0,1187	0,0989	120,3	2,019
	2	16,8	1280	0,099	0,0825	120,3	2,019
	3	24,65	1270	0,1017	0,0848	120,4	2,02

	4	23,66	1280	0,1398	0,1165	120,3	2,019
	5	22,77	1140	0,1261	0,1051	120,3	2,019
	6	–	1430	0,1283	0,1069	120,3	2,018
	7	–	1150	0,1271	0,1059	120,3	2,019
	8	–	1350	0,1361	0,1134	120,3	2,018
	AVERAGE	20,452	1281,25	0,1221	0,10175	120,3125	2,018875
	STD_DEV	4,56874928	99,2021745	0,01488076	0,01238801	0,03535534	0,00064087
	STD ERROR	2,04320679	35,0732652	0,00526114	–	–	–
	EQUIP ERROR	0,61356	128,125	0,002221	–	–	–
	TOTAL ERROR	2,13334242	132,83881	0,00571073	–	–	–
DIESTER	**PROPERTIES**	**BDV**	**Rho**	**Tan delta 50Hz**	**Tan delta 60Hz**	**C**	**e**
	UNITS	**KV**	**G Ohm*m**	**%**	**%**	**pF**	
	1	60,06	8,79	6,6728	5,5607	206	3,456
	2	64,35	9,26	3,6672	3,056	206,8	3,469
	3	71,86	9,57	3,4518	2,8765	206,5	3,465
	4	61,94	9,9	3,6106	3,0088	206,2	3,46
	5	64,35	10,6	3,2935	2,7445	206,3	3,462
	6	–	10,4	3,1103	2,5919	206,6	3,466
	7	–	10,2	3,1592	2,6326	206,1	3,458
	8	–	10,3	3,2831	2,7359	206,2	3,46
	AVERAGE	64,512	9,8775	3,7810625	3,1508625	206,3375	3,462
	STD_DEV	4,4855624	0,62524852	1,18532098	0,98779203	0,27222627	0,00437526
	STD ERROR	2,00600449	0,22105873	0,41907425	–	–	–

	EQUIP ERROR	1,93536	0,98775	0,03881063	–	–	–
	TOTAL ERROR	2,7874132	1,01218428	0,42086755	–	–	–
POLYOLESTER	**PROPERTIES**	**BDV**	**Rho**	**Tan delta 50Hz**	**Tan delta 60Hz**	**C**	**e**
	UNITS	**KV**	**G Ohm*m**	**%**	**%**	**pF**	
	1	57,82	31,7	1,0985	0,9154	183,3	3,075
	2	42,72	26,2	0,7735	0,6446	183,7	3,082
	3	68,86	27,2	0,844	0,7033	183,5	3,078
	4	78,28	27,6	0,878	0,7317	183,2	3,073
	5	79,86	21,7	1,7074	1,4228	183,2	3,073
	6		28,4	1,2242	1,0202	183,1	3,072
	7		29,1	1,1779	0,9816	182,8	3,067
	8		31,4	1,0809	0,9007	183,1	3,072
	AVERAGE	65,508	27,9125	1,09805	0,9150375	183,2375	3,074
	STD_DEV	15,481748	3,16879315	0,29572857	0,24643168	0,27222627	0,00447214
	STD ERROR	6,92364817	1,12033756	0,10455584	–	–	–
	EQUIP ERROR	1,96524	2,79125	0,0119805	–	–	–
	TOTAL ERROR	7,19715723	3,0076956	0,10523999	–	–	–
5W30	**PROPERTIES**	**BDV**	**Rho**	**Tan delta 50Hz**	**Tan delta 60Hz**	**C**	**e**
	UNITS	**KV**	**G Ohm*m**	**%**	**%**	**pF**	
	1	42,02	0,0113	16,339	13,615	128,1	2,149
	2	37,52	0,01	17,467	14,556	127,9	2,146
	3	46,25	0,00966	16,598	13,831	128,3	2,153

	4	54,52	0,00991	16,535	13,779	127,9	2,146
	5	43,43	0,00939	20,022	16,685	128,7	2,16
	6	21,79	0,00919	19,636	16,363	128,9	2,163
	7	–	0,00912	19,031	15,859	129	2,164
	8	–	0,00897	18,66	15,55	128,8	2,162
	AVERAGE	40,9216667	0,0096925	18,036	15,02975	128,45	2,155375
	STD_DEV	10,9397978	0,0007484	1,48362548	1,23653072	0,45355737	0,00774481
	STD ERROR	4,46615376	0,0002646	0,52454082	–	–	–
	EQUIP ERROR	1,22765	0,00096925	0,18136	–	–	–
	TOTAL ERROR	4,63180893	0,00100472	0,55500858	–	–	–

Table B-5: Raw data for electrical properties of the thermally aged oil samples.

	THERMALLY AGED						
Group III	**PROPERTIES**	**BDV**	**Rho**	**Tan delta 50Hz**	**Tan delta 60Hz**	**C**	**e**
	UNITS	**KV**	**G Ohm*m**	**%**	**%**	**pF**	
	1	26,6349756	103,00	1,24	1,03	122,80	2,06
	2	22,4034555	94,00	1,16	0,97	122,70	2,06
	3	24,9076001	98,00	1,02	0,85	122,80	2.06
	4	18,686998	90,00	1,44	1,20	122,70	2,06
	5	25,1669708	101,00	1,14	0,95	122,80	2,06
	6	–	101,00	1,06	0,89	122,80	2,06
	7	–	103,00	1,06	0,88	122,80	2,06
	8	–					

	AVERAGE	23,56	98,5714286	1,16084286	0,96738571	122,771429	2,06
	STD_DEV	3,12	4,9280538	0,14485524	0,12069947	0,048795	0
	STD ERROR	1,39530642	1,86262926	0,05475013	–	–	–
	EQUIP ERROR	0,7068	9,85714286	0,01260843	–	–	–
	TOTAL ERROR	1,56411197	10,0315828	0,05618318	–	–	–
PAO	**PROPERTIES**	**BDV**	**Rho**	**Tan delta 50Hz**	**Tan delta 60Hz**	**C**	**e**
	UNITS	**KV**	**G Ohm*m**	**%**	**%**	**pF**	
	1	21,4280158	1040	0,1958	0,1631	121,9	2,046
	2	21,57465	1010	0,1643	0,1369	121,9	2,046
	3	26,1211214	1060	0,1604	0,1336	122	2,046
	4	23,8489086	1000	0,1724	0,1436	122,1	2,049
	5	20,9773042	1100	0,1871	0,1559	122,1	2,049
	6	–	–	–	–	–	–
	7	–	–	–	–	–	–
	8	–	–	–	–	–	–
	AVERAGE	22,79	1042	0,176	0,14662	122	2,0472
	STD_DEV	2,17	40,2492236	0,01507034	0,01255814	0,1	0,00164317
	STD ERROR	0,9704535	18	0,00673966	–	–	–
	EQUIP ERROR	0,6837	104,2	0,00276	–	–	–
	TOTAL ERROR	1,18710812	105,743274	0,0072829	–	–	–
DIESTER	**PROPERTIES**	**BDV**	**Rho**	**Tan delta 50Hz**	**Tan delta 60Hz**	**C**	**e**

	UNITS	**KV**	**G Ohm*m**	**%**	**%**	**pF**	
	1	51,97	2,95	11	9,1691	207,7	3,484
	2	65,79	2,72	11,476	9,5639	207,3	3,479
	3	63,19	2,74	9,9726	8,3105	207,5	3,481
	4	54,2	2,83	9,8678	8,2231	207,1	3,475
	5	69,63	–	–	–	–	–
	6	–	–	–	–	–	–
	7	–	–	–	–	–	–
	8	–	–	–	–	–	–
	AVERAGE	60,956	2,81	10,5791	8,81665	207,4	3,47975
	STD_DEV	7,5826829	0,10488088	0,78642151	0,65602159	0,25819889	0,00377492
	STD ERROR	3,39107888	0,05244044	0,39321075	–	–	–
	EQUIP ERROR	1,82868	0,281	0,106791	–	–	–
	TOTAL ERROR	3,85272456	0,28585136	0,40745431	–	–	–
POLYOLESTER	**PROPERTIES**	**BDV**	**Rho**	**Tan delta 50Hz**	**Tan delta 60Hz**	**C**	**e**
	UNITS	**KV**	**G Ohm*m**	**%**	**%**	**pF**	
	1	63,67	11,5	1,8564	1,547	185,1	3,106
	2	59,32	11,4	1,78	1,4833	185,1	3,105
	3	63,48	11,7	1,8375	1,5313	184,8	3,1
	4	58,36	11	1,8948	1,579	184,9	3,102
	5	48,96	11,7	1,8374	1,5311	184,9	3,102
	6	–	–	–	–	–	–
	7	–	–	–	–	–	–
	8	–	–	–	–	–	–

	AVERAGE	58,758	11,46	1,84122	1,53434	184,96	3,103
	STD_DEV	5,97704107	0,28809721	0,04146555	0,03456737	0,13416408	0,00244949
	STD ERROR	2,67301403	0,12884099	0,01854396	–	–	–
	EQUIP ERROR	1,76274	1,146	0,0194122	–	–	–
	TOTAL ERROR	3,20191448	1,15321984	0,02684608	–	–	–
5W30	**PROPERTIES**	**BDV**	**Rho**	**Tan delta 50Hz**	**Tan delta 60Hz**	**C**	**e**
	UNITS	**KV**	**G Ohm*m**	**%**	**%**	**pF**	
	1	45,95	0,00345	38,508	32,09	89,7	1,504
	2	39,8	0,00353	37,968	31,64	90,83	1,523
	3	51,55	0,00355	38,792	32,327	89,01	1,493
	4	26,08	0,00353	39,411	32,843	87,87	1,474
	5	29,11	0,00356	40,12	33,433	86,52	1,451
	6	31,19	0,00328	39,667	33,056	87,24	1,463
	7	–	0,00333	39,567	32,973	87,52	1,468
	8	–	0,00337	39,267	32,723	88,01	1,476
	AVERAGE	37,28	0,00345	39,1625	32,635625	88,3375	1,4815
	STD_DEV	10,1432657	0,00010994	0,69694128	0,58078861	1,41538233	0,02360993
	STD ERROR	4,1409709	3,8868E-05	0,24640595	–	–	–
	EQUIP ERROR	1,1184	0,000345	0,392625	–	–	–
	TOTAL ERROR	4,28934244	0,00034718	0,46354103	–	–	–

Table B-6: Raw data for electrical properties of the electrically aged oil samples.

	ELECTRICALLY AGED						
Group III	**PROPERTIES**	**BDV**	**Rho**	**Tan delta 50Hz**	**Tan delta 60Hz**	**C**	**e**
	UNITS	**KV**	**G Ohm*m**	**%**	**%**	**pF**	
	1	27,32	288	0,538	0,4483	121,4	2,036
	2	23,16	268	0,6347	0,5289	121,3	2,04
	3	20,22	337	0,6233	0,5194	121,2	2,03
	4	23,66	295	0,8512	0,7093	121,4	2,04
	5	24,35	418	0,4521	0,3767	121,6	2,04
	6	–	410	0,5039	0,4199	121,5	2,039
	7	–	383	0,4365	0,3637	121,4	2,037
	8	–	343	0,8201	0,6834	121,4	2,036
	AVERAGE	23,742	342,75	0,607475	0,5062	121,4	2,03675
	STD_DEV	2,54566691	56,9504797	0,157902	0,13159222	0,11952286	0,00212132
	STD ERROR	1,13845685	20,1350352	0,05582679	–	–	–
	EQUIP ERROR	0,71226	34,275	0,00707475	–	–	–
	TOTAL ERROR	1,34290666	39,75167	0,05627328	–	–	–
PAO	**PROPERTIES**	**BDV**	**Rho**	**Tan delta 50Hz**	**Tan delta 60Hz**	**C**	**e**
	UNITS	**KV**	**G Ohm*m**	**%**	**%**	**pF**	
	1	21,18	1360	0,1436	0,1197	120,8	2,026
	2	38,61	1450	0,1574	0,1311	120,4	2,021
	3	30,39	1500	0,153	0,1275	120,5	2,022
	4	35,84	1555	0,1744	0,1454	120,3	2,019

	5	29,5	1680	0,1266	0,1055	120,6	2,024
	6		1530	0,1843	0,1536	120,3	2,019
	7		1680	0,154	0,1283	120,8	2,026
	8						
	AVERAGE	31,104	1536,42857	0,15618571	0,13015714	120,528571	2,022428571
	STD_DEV	6,71450147	116,573092	0,01902756	0,01586735	0,21380899	0,002992053
	STD ERROR	3,00281634	44,0604872	0,00719174	–	–	–
	EQUIP ERROR	0,93312	153,642857	0,00256186	–	–	–
	TOTAL ERROR	3,14445845	159,83571	0,00763441	–	–	–
DIESTER	**PROPERTIES**	**BDV**	**Rho**	**Tan delta 50Hz**	**Tan delta 60Hz**	**C**	**e**
	UNITS	**KV**	**G Ohm*m**	**%**	**%**	**pF**	
	1	21,68	5,98	7,0511	5,8759	206,5	3,465
	2	29,11	7,79	4,9147	4,0956	207,8	3,487
	3	27,5	7,79	4,9439	4,1199	206,8	3,469
	4	28,02	8,41	3,9853	3,3127	206,4	3,463
	5	24,85	8,37	4,5717	3,8098	206,7	3,468
	6		8,7	3,8226	3,1855	206,4	3,463
	7		9,09	3,5632	2,9693	206,3	3,462
	8		9,23	3,5029	2,919	206,2	3,46
	AVERAGE	26,232	8,17	4,544425	3,7859625	206,6375	3,467125
	STD_DEV	2,98823861	1,03049225	1,16263717	0,96945425	0,50972682	0,008576338
	STD ERROR	1,33638093	0,36433403	0,41105431	–	–	–
	EQUIP ERROR	0,78696	0,817	0,04644425	–	–	–

	TOTAL ERROR	1,55087718	0,8945548	0,41366981	–	–	–
POLYOLESTER	**PROPERTIES**	**BDV**	**Rho**	**Tan delta 50Hz**	**Tan delta 60Hz**	**C**	**e**
	UNITS	**KV**	**G Ohm*m**	**%**	**%**	**pF**	
	1	35,84	16,3	2,7173	2,2644	183,1	3,072
	2	24,35	12,9	1,5923	1,3269	183,3	3,076
	3	37,92	14,3	1,3055	1,0879	183,8	3,083
	4	37,52	13,2	1,377	1,1475	183,4	3,077
	5	36,73	13,7	2,0198	1,6831	183,5	3,079
	6		17,4	1,5385	1,282	183,2	3,074
	7		17,9	1,4998	1,2499	183,2	3,073
	8		14,7	1,3947	1,1622	183,9	3,085
	AVERAGE	34,472	15,05	1,6806125	1,4004875	183,425	3,077375
	STD_DEV	5,71410273	1,91833261	0,47284749	0,39403412	0,29154759	0,004688512
	STD ERROR	2,55542443	0,678233	0,16717683	–	–	–
	EQUIP ERROR	1,03416	1,505	0,01780613	–	–	–
	TOTAL ERROR	2,75675188	1,65076497	0,16812243	–	–	–
5W30	**PROPERTIES**	**BDV**	**Rho**	**Tan delta 50Hz**	**Tan delta 60Hz**	**C**	**e**
	UNITS	**KV**	**G Ohm*m**	**%**	**%**	**pF**	
	1	56,65	0,00726	25,698	21,415	120,1	2,016
	2	46,19	0,00723	25,59	21,325	120,8	2,026
	3	43,94	0,00682	26,368	21,973	118,6	1,99
	4	39,01	0,0071	26,14	21,784	118,9	1,996

	5	33,17	0,00811	23,762	19,801	124,3	2,085
	6	34,75	0,00809	22,889	19,074	125,8	2,11
	7	–	0,00802	21,791	18,159	126,1	2,116
	8	–	0,00857	20,821	17,351	125,8	2,111
	AVERAGE	42,285	0,00765	24,132375	20,11025	122,55	2,05625
	STD_DEV	8,65940356	0,00062202	2,12921279	1,77440346	3,26846403	0,054559928
	STD ERROR	3,5351867	0,00021992	0,7527904	–	–	–
	EQUIP ERROR	1,26855	0,000765	0,24232375	–	–	–
	TOTAL ERROR	3,75589724	0,00079598	0,79083133	–	–	–